Synthesis, Spectroscopy, and Molecular Orbital Calculations of Subazaporphyrins, Subphthalocyanines, Subnaphthalocyanines, and Compounds Derived Therefrom by Ring Expansion[1]

Nagao Kobayashi,*,† Takeo Ishizaki,† Kazuyuki Ishii,† and Hideo Konami‡

Contribution from the Department of Chemistry, Graduate School of Science, Tohoku University, Sendai 980-8578, Japan, and Miyagi National College of Technology, Natori 981-1239, Japan

Received September 17, 1998

Abstract: A subazaporphyrin (SubAP), *tert*-butylated and crowned subphthalocyanines (tBSubPc and SubCRPc), a μ-oxo dimer of *tert*-butylated SubPc {$(tBSubPc)_2O$}, a subnaphthalocyanine (SubNc), and monosubstituted type unsymmetrical phthalocyanine (Pc) and naphthalocyanine (Nc) analogues have been synthesized. In particular, unsymmetrical Pc's and Nc's have been prepared in moderate yields by the ring expansion reaction of structurally distorted SubPc's and SubNc's with isoindolediimine derivatives in dimethyl sulfoxide−chloronaphthalene (or chlorobenzenes or aromatic hydrocarbons such as toluene and xylene) mixtures. The compounds have been characterized by electronic absorption, magnetic circular dichroism (MCD), fluorescence emission, and nuclear magnetic resonance spectroscopy. Both the Soret bands and Q-bands shift to longer wavelength and gain intensity in the order SubAP, SubPc, and SubNc. Fluorescence quantum yields and lifetimes generally decrease with decreasing molecular symmetry. Circular dichroism and NMR spectroscopy have revealed that a SubPc with three 15-crown-5 ether voids having a phenyl group as an axial ligand (SubCRPc) forms inclusion complexes with 2,6-dimethyl-β-cyclodextrin in acetonitrile or water−acetonitrile mixtures, while the electronic absorption spectroscopy suggests that it is not dimerized by the addition of cations such as K^+, Rb^+, Ce^+, i.e., cations which are effective in dimerizing Pc's with 15-crown-5 ether voids. Molecular orbital (MO) calculations within the framework of the Pariser−Parr−Pople approximation have succeeded in reproducing the optical absorption experimental data of not only the parent subazamacrocycles but also Pc derivatives with lower symmetry obtained by the ring expansion reaction. The correspondence between MO calculations and experiments suggests strongly that, in the metal-free unsymmetrical Pc's, two pyrrole hydrogen atoms are bound to the nitrogens along the short axis. Comparison of formation, bonding, and donation energies between SubPc and typical Pc, i.e., MgPc by natural bond orbital analysis, suggests that the distortion energy is not the major reason for the ring expansion reactivity of SubPc, and that the lack of donor−acceptor stabilization in B−N(pyrrole) bonds destabilizes SubPc. Band deconvolution of the electronic absorption and MCD spectra of SubPc with the same set of bands (with the same centers and width) experimentally identified that the excited state of the Q-band of SubPc is orbitally degenerate, with three degenerate transitions located in the 250−450-nm region. In particular, the transition at 359 nm corresponds to a shoulder seen on the red side of the Soret band tail. Time-resolved EPR analysis has shown that the size of the π-system of SubPc is, indeed, smaller than that of Pc's.

Introduction

In 1990, we reported a new method for preparing monosubstituted type phthalocyanines (Pc's) via the so-called subphthalocyanines (SubPc's).[1] Among various Pc analogues, monosubstituted C_{2v} type Pc's had previously been prepared either by mixed condensation reaction[2] or by a polymer support[3] method. The former method gave mixtures of products that could not be readily separated by chromatographic methods, while the latter method required a functional group which is linked to a polymer and which could be cleaved therefrom after synthesis. Following our introduction of this new method, several groups have reported many new monosubstituted type Pc's.[4] However, most papers have been concerned only with the synthesis of SubPc's, and the spectroscopic characterization of these compounds has not been examined in detail. In this

† Tohoku University.

‡ Miyagi National College of Technology.

(1) Preliminary results have been published: Kobayashi, N.; Kondo, R.; Nakajima, S.; Osa, T. *J. Am. Chem. Soc.* **1990**, *112*, 9640.

(2) (a) Konami, H.; Hatano. H. *Chem. Lett.* **1988**, 1359. (b) Piechocki, C.; Simon, J. *J. Chem. Soc., Chem. Commun.* **1985**, 259.

(3) Leznoff, C. C. In *Phthalocyanines—Properties and Applications*; Leznoff, C. C., Lever, A. B. P., Eds.; VCH: New York, 1989; Chapter 1.

(4) (a) Kobayashi, N. *J. Chem. Soc., Chem. Commun*. **1991**, 1203. (b) Musluoglu, E.; Gurec, A.; Ahsen, V.; Gul, A.; Bekaroglu, O. *Chem. Ber*. **1992**, *125*, 2337. (c) Kasuga, K.; Idehara, T.; Hamada, M.; Isa, K. *Inorg. Chim. Acta* **1992**, *196*, 127. (d) Danak, S.; Gul, A.; Bekaloglu, O. *Chem. Ber*. **1994**, *127*, 2009. (e) Hanack, M.; Geyer, M. *J. Chem. Soc., Chem. Commun*. **1994**, 2253. (f) Rauschnabel, J.; Hanack, M. *Tetrahedron Lett*. **1995**, 1629. (g) Weitmeyer, A.; Kliesch, H.; Wohrle, D. *J. Org. Chem*. **1995**, *60*, 4900. (h) Sastre, A.; Torres, A.; Hanack, M. *Tetrahedron Lett*. **1995**, 8501. (i) Diaz-Garcia, M. A.; Agullo-Lopez, F.; Sastre, A.; Torres, T.; Torruellas, W. E.; Stegeman, G. I. *J. Phys. Chem*. **1995**, *99*, 14988. (j) Sastre, A.; Torres, T.; Diaz-Garcia, M. A.; Agullo-Lopez, F.; Dhenaut, C.; Brasselet, S.; Ledoux, I.; Zyss, J. *J. Am. Chem. Soc*. **1996**, *118*, 2746. (k) Sastre, A.; Rey, B.; Torres, T. *J. Org. Chem*. **1996**, *61*, 8591. (l) Geyer, M.; Plenzig, F.; Rauschnabel, J.; Hanack, M.; Rey, B.; Sastre, A.; Torres, T. *Synthesis* **1996**, 1139. (m) Kasuga, K.; Idehara, T.; Handa, M.; Ueda, Y.; Fujiwara, T.; Isa, K. *Bull. Chem. Soc. Jpn.* **1996**, *69*, 2559. (n) Kudrevich, S.; Brasseur, N.; Madeleine, C. L.; Gilbert, S.; van Lier, J. E. *J. Med. Chem.* **1997**, *40*, 3897.

10.1021/ja983325c CCC: $18.00
Published on Web 09/15/1999

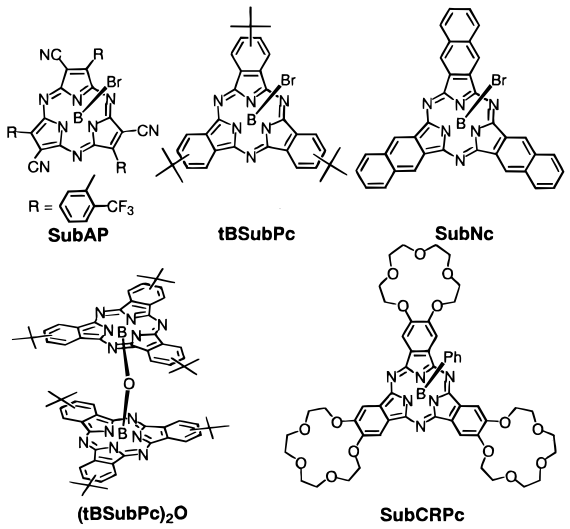

Figure 1. Structures and abbreviations of the subazamacrocycles studied.

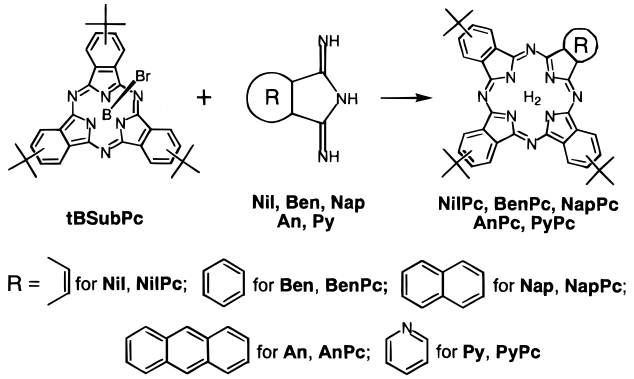

Figure 2. Synthetic routes to various low-symmetrical Pc derivatives NilPc−PyPc from tBSubPc. The resultant Pc derivatives are expressed using abbreviations of the molecules introduced. BenPc, NapPc, AnPc, and PyPc represent, therefore, a benzene-, naphthalene-, anthracene-, and pyridine unit-introduced Pc, respectively, while NilPc means Pc analogue without fused ring.

paper, we have initially synthesized a subazaporphyrin (SubAP), several SubPc's, and a subnaphthalocyanine (SubNc) (Figure 1) and then further obtained new compounds by ring expansion reaction of these (Figure 2). Most of the new compounds have been characterized by various spectroscopic techniques, and some of the data has been reproduced by molecular orbital (MO) calculations. We have also considered, through quantum chemical calculations, why SubPc's can be utilized for ring expansion reactions.

Results and Discussion

I. Synthesis and NMR. (a) SubAP, tBSubPc, SubNc, $(tBSubPc)_2O$, and SubCRPc. Syntheses of normal SubPc's have been reported in several publications.[4] Accordingly, we comment here only on the syntheses of SubAP, SubNc, and crowned subphthalocyanines (SubCRPc). As a starting material for SubAP, we used 2-(*o*-trifluoromethyl)phenyl-1,1,2-tricyanoethylene because of (i) its accessibility,[5] (ii) the high solubility we expected for the resulting macrocycles, (iii) the low temperature that we expected cyclization to require, (iv) the low possibility of bromination during cyclization with boron tribromide, and (v) the small substituent effect we anticipated on the electronic absorption spectra of the product.[5] The desired SubAP suitable for spectroscopic study was synthesized without bromination, although the yield was not high (1.9%).

Substituent-free SubNc was initially synthesized from 2,3-dicyanonaphthalene and BBr_3 in chloronaphthalene according to the procedure reported by Meller and Ossko.[6] The problem of partial bromination was greatly diminished when 6-*tert*-butyl-2,3-dimethylnaphthalene, obtained by Friedel−Crafts butylation of 2,3-dimethylnaphthalene, was used as a solvent, since bromination occurred mostly on this compound due to electron-rich character of the molecule.

To synthesize $(SubPc)_2O$, we first changed the axial bromine atom of *tert*-butylated subphthalocyanines (tBSubPc's) to an OH group using an ion-exchange resin,[7] and the resultant tBSubPc with the OH group was heated at ca. 200 °C under vacuum for 21 h. After cooling, the residue was imposed on a gel permeation chromatography column for complete separation from the monomeric tBSubPc.

Boron tribromide is an effective cutter of ether linkages.[8] Accordingly, triphenylborane[4e] was used instead of BBr_3 for the synthesis of SubCRPc, to avoid cleavage of the crown ether unit. The reaction was carried out in naphthalene in the presence of 1,8-diazabicyclo[5,4,0]-7-undecene (DBU), but the yield was very low (ca. 0.4%). This low yield is ascribed to the difficulty of the elimination of two phenyl groups from triphenylborane. Even with such a low yield, SubCRPc is requisite for the cation complexation studies (for details, see section III).

NMR signals of protons of tBSubPc were observed at 8.63−8.71 (m, 3H, arom), 8.50−8.56 (m, 3H, arom), 7.82−7.90 (m, 3H, arom), and 1.48−1.57 ppm (m, 27H, butyl). The positions of these signals did not change at $0.07 < [tBSubPc] < 5$ mM, suggesting that the aggregation trend is very small.[9] In comparison with these, in the corresponding zinc phthalocyanine, i.e., tetra-*tert*-butylphthalocyaninatozinc(II) (tBZnPc), the corresponding proton signals appear at 8.3−8.9 (br, 8H, arom), 7.90−8.08 (br, 4H, arom), and 1.72−1.77 ppm (m, 36H, butyl) at 0.1 mM. Although there is almost no difference in the positions of aromatic proton signals between tBSubPc and tBuZnPc, the position of *tert*-butyl protons suggests that the ring current of a SubPc skeleton is smaller than that of the Pc skeleton.

(b) Unsymmetrical Pc Analogues. Monosubstituted type Pc analogues (Figure 2) were obtained by reacting tBSubPc[4a] (1 equiv) and 1*H*-isoindole-1,3(2*H*)-diimine[10] or its analogues Nil, Ben, Nap, An, or Py (typically ca. 7 equiv) at 80−90 °C in a mixture of dimethyl sulfoxide (DMSO) and either chlorobenzene, dichlorobenzene, toluene, xylene, or 1-chloronaphthalene (CNP) (mostly 5:1−1:3 v/v) for 5−30 h (Figure 3). To find the optimum solvent ratio in the reaction, the solvent ratio was continuously varied (from 10:0 to 0:10 v/v) between DMSO and CNP, and the above experiments were repeated at fixed [SubPc] and [isoindolediimine], keeping other conditions exactly the same. We were unable to obtain any BenPc in pure DMSO or CNP. However, when the more soluble 5-*tert*-butyl-1*H*-

(5) Troitskaya, V. I.; Trushanina, L. A.; Kopranenkov, V. N.; Luk'yanets, E. A.; Yagupol'skii, L. M. *J. Gen. Chem. (Engl. Transl.)* **1989**, *25*, 513.

(6) (a) Meller, A.; Ossko, A. *Monatsh. Chem.* **1972**, *103*, 150. (b) Kietaibl, H. *Monatsh. Chem.* **1974**, *105*, 405.

(7) Sauer, T.; Wegner, G. *Mol. Cryst. Liq. Cryst.* **1988**, *162B*, 97.

(8) McOmie, J. F.; Watts, M. L.; West, D. E. *Tetrahedron* **1968**, *24*, 2289. Bhatt, M. V.; Kulkarnyi, S. U. *Synthesis* **1983**, 249.

(9) Positions of NMR signals of Pc's change on aggregation: Terekhov, D. S.; Nolan, K. L. M.; McArthur, C. R.; Leznoff, C. C. *J. Org. Chem.* **1996**, *61*, 3034.

(10) 1*H*-Isoindole-1,3(2*H*)-diimine and its analogues were obtained by reacting aromatic *ortho*-dinitriles with ammonia gas in dry methanol or propanol containing CH_3ONa or C_2H_5ONa (Brach, P. J.; Grammatica, S. J.; Ossanna, O. A.; Weinberger, L. *J. Heterocycl. Chem.* **1970**, *7*, 1403).

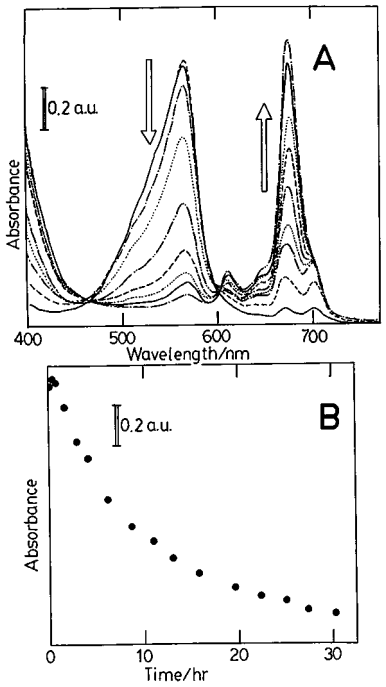

Figure 3. (a) Spectroscopic change during the reaction of tSubPc and *tert*-butylisoindolediimine in a 1:1 (v/v) mixture of DMSO and CNP at 90 °C. [tSubPc]/M = 2.21×10^{-5} and [*tert*-butylisoindolediimine]/M = 1.44×10^{-3}. Arrows indicate the direction of spectroscopic change. (b) Absorbance change at 570 nm with time, replotted from (a).

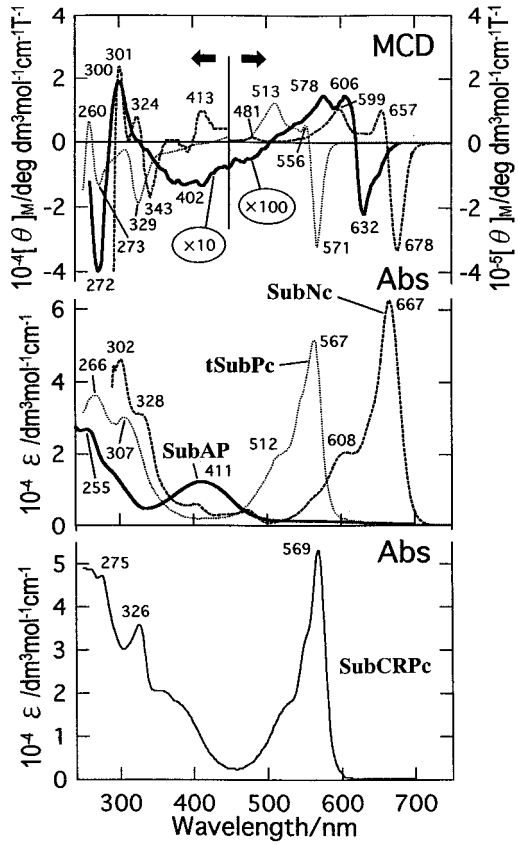

Figure 4. MCD (top) and electronic absorption (middle) spectra of SubAP (—), tBSubPc (· · ·), and SubNc (- - -) in $CHCl_3$ (the former two) or in *o*-dichlorobenzene (the latter one). The bottom panel shows the electronic absorption spectrum of SubCRPc in $CHCl_3$.

isoindole-1,3(2*H*)-diimine was employed instead of the less soluble 1*H*-isoindole-1,3(2*H*)-diimine, the reaction proceeded even in pure DMSO or CNP, and some tetra-*tert*-butylated H_2-Pc was obtained. Accordingly, the solubility of the reactant is important, as in general reactions. Next, we repeated the same experiment using isoindolediimine derivatives Nil and Nap. Again, the reaction did not proceed in the two single solvents, and the optimum solvent ratio changed from system to system. However, *relatively good yields were attained in the range of DMSO:CNP = 3:1−1:2 v/v.*

The formation of tetra-*tert*-butylated H_2Pc from tBSubPc and 5-*tert*-butyl-1*H*-isoindole-1,3(2*H*)-diimine was monitored spectroscopically (Figure 3A). The 570-nm band of tSubPc disappears with concomitant increase of the absorption at ca. 600−720 nm. The time evolution of this reaction is plotted in Figure 3B by following the change of absorbance at 570 nm. The absorbance changes relatively rapidly initially, but the rate decreases as the reaction proceeds, and it takes almost 1 day to complete the reaction.

Pyrrole proton signals of porphyrins and Pc's generally appear at around −2 to −6 ppm,[11] and their position is an approximate measure of the strength of the ring current. In the order of NilPc to PyPc, the NH proton signals of 0.1 mM solution appeared at −1.73 to −1.97, −2.7 to −4.1, −2.35 to −3.2, −1.8 to −4.4, and −2.3 to −2.8 ppm, respectively. In the case of Pc's, the position of the proton signals depends on the degree of aggregation.[9] However, considering that *tert*-butyl groups reduce the aggregation[9] and that the sizes of the π-systems of NilPc to PyPc, which affect the degree of aggregation, do not differ significantly, the above data at 0.1 mM concentration appear to be directly comparable. Signals of BenPc emerged at the highest field, indicating that the ring current in this complex is the largest. Elimination of a benzene ring from BenPc (i.e., NilPc) or fusion of another benzene (i.e., NapPc) reduces the ring current. In particular, the ring current of NilPc is much smaller than that of BenPc, suggesting that the main contribution to the Pc ring current is not only from the inner 16- or 20-membered rings but also from the four benzene rings. According to theoretical calculations on π-electron ring currents of porphyrins and Pc's,[12] in tetrabenzoporphyrins and Pc's the ring current along the outer rim, including four benzene rings, is predicted to exceed that along the inner 20-membered porphyrin skeleton. Hence, the small ring current in NilPc compared to that in BenPc may be in accord with this prediction. The slight downfield shift of signals of NapPc and AnPc from BenPc indicates that the further outer fused benzenes have a slight effect on the ring current of the macrocycles. Comparison of the position of the NH proton signals of BenPc (−2.7 to −4.1 ppm) and PyPc (−2.3 to −2.8 ppm) reveals that fusion of a heterocyclic aromatic ring in place of a benzene ring also reduces the ring current in Pc's.[13]

II. Spectroscopy. (i) Electronic Absorption and Magnetic Circular Dichroism Spectroscopy. (a) SubAP, tBSubPc, SubNc, $(tBSubPc)_2O$, and SubCRPc. The electronic absorption and magnetic circular dichroism (MCD) spectra of SubAP, tBSubPc, and SubNc in this study (Figure 4) clearly indicate a tendency for both the Soret bands and Q-bands to shift to longer

(11) Leznoff, C. C.; Marcuccio, S. M.; Greenberg, S.; Lever, A. B. P.; Tomer, K. B. *Can. J. Chem.* **1985**, *63*, 623, 3057. Scheer, H.; Katz, J. J. In *Porphyrins and Metalloporphyrins*; Smith, K. M., Ed.; Elsevier: Amsterdam, New York, 1975; Chapter 10.

(12) Vysotsky, Y. B.; Kuzmitsky, V. A.; Solovyov, K. N. *Theor. Chim. Acta (Berin)* **1981**, *59*, 467.

(13) In fact, tetrapyradinoporphyrazines show the NH proton signals at −1.2 to −1.5 ppm in chloroform (Tokita, S.; Kojima, M.; Kai, N.; Nishi, H.; Tomoda, H.; Saito, S.; Shiraishi, S. *Nihon Kagaku Kaishi* **1990**, 219).

wavelengths and intensify with the increase of the π-conjugation system. The SubAP, tBSubPc, and SubNc have Q-bands at 411 (pale brown), 567 (reddish-purple), and 667 nm (greenish-blue) and Soret bands at ca. 290, 307, and 328 nm, respectively. Compared with the band positions of the corresponding cyclic tetramers, i.e., *tert*-butylated TAP, Pc, and Nc, in the same solvent,[14] the Q-bands are shifted to the blue by ca. 170−180 (ca. 7100−7400 cm^{-1}), 120−130 (ca. 3000−3500 cm^{-1}), and 100−120 nm (ca. 2000−2340 cm^{-1}), respectively, and the Soret bands ca. 40−50 nm (ca. 4200−5100 cm^{-1}), 23−33 nm (ca. 2300−3200 cm^{-1}), and 5−15 nm (ca. 500−1300 cm^{-1}), respectively. These data indicate that, although the bands shift to longer wavelength with the fusion of the benzene unit, the extent of the shift becomes smaller as the size of the molecule increases.

It is also interesting to compare the band position among SubPc, Pc, and superphthalocyanines (SPc's),[15] i.e. for cyclic trimers, tetramers, and pentamers of isoindolediimines having the same or similar substituent groups. Considering that the Q-band of SPc's appears at ca. 910−930 nm, it is found that the Q-band energy changes ca. 3000−3600 cm^{-1} per isoindolediimine unit. Absorption coefficients (ϵ) in both the Soret bands and Q-bands also increase on going from SubPc's to Pc's. For example, the ϵ values of the Q-bands of alkylated SubPc's are (5−6) $\times$ 10^4 dm^3 mol^{-1} cm^{-1}, as seen for tBSubPc and SubCRPc in Figure 4, and those of most Pc's[14] are in the range (8−24) $\times$ 10^4 dm^3 mol^{-1} cm^{-1}. The Q-band of SPc's may be weaker since the area of the Q-band is smaller when the abscissa of the spectrum is expressed in cm^{-1} unit. A severe buckling structure of SPc[15c] may prevent a large transition moment from being produced. The smaller Q-band intensity of SubPc's compared to that of general Pc's may be attributed to their nonflat, cone-shaped structure.[6b] Under such circumstances, transition moments, which can be expressed by linear vectors, cannot become large.

The absorption spectrum of SubCRPc is different from that of tBSubPc in that another envelope is involved at the longer wavelength side of the Soret band. This band has been postulated to be an n−π transition in ether oxygen or thioether sulfur.[16,17] However, the band appears much more intense than n−π transitions, suggesting strong intensity borrowing from the π-system.

Given the somewhat cone-shaped nature of SubPc's,[6b] the MCD spectra of these subazacompounds can be interpreted under the C_{3v} or D_{3h} approximation. The Q-band MCD spectra of tBSubPc and SubNc appear to correspond to the wavelengths of the absorption spectra. Though the spectra are not symmetrical with respect to the line of $[\theta]_M = 0$, this nonsymmetricity is due to the superimposition of Faraday *A* and *B* terms, as will be shown later in the sections on MO calculations and band deconvolution. Namely, a transition to the degenerate state is included in this region, as in general metalloPc's.[18] In the 250−350-nm region of the spectra of tBSubPc, two dispersion type MCD curves are observed, corresponding to two absorption peaks. These are also transitions to the doubly degenerate excited states (see MO section).

Table 1 summarizes the most important electronic absorption and MCD data in the Q-band. Apparently, the dipole strength of SubNc is almost the same as those of BenPc, NapPc, and PyPc (Table 1A). However, this indicates that the intensity of the Q-band of SubNc is about half those of the latter compounds, since the values for BenPc, NapPc, and PyPc are only for the Q_{x0-0} band. Since the value for tBSubPc is even smaller, we can conclude safely that the Q-bands of subaza compounds are weaker than those of the corresponding tetrapyrrolytic Pc's or Nc's. In addition, *A/D* values and magnetic moments (μ) in Table 1B are also smaller than those of Pc's, indicating that the orbital angular momentum of the excited state of the subazamacrocyclic ligand is smaller than that of Pc's.[18]

The spectra of $(tBSubPc)_2O$ are collected in Figure 5. Compared with the spectrum of the constituting monomer, tBSubPc, the Q-band shifts to the blue, while the position of the Soret band is virtually the same. The blue-shift of the Q-band can be explained on the basis of an exciton interaction. Also, the shape of the Q-band is similar to that of the μ-oxo-dimer of an iron Pc,[19] though both the Q-bands and Soret bands appear at shorter wavelengths than the respective band of the Pc's.

(b) Unsymmetrical Pc Analogues. Electronic absorption and MCD spectra of NilPc to PyPc are collected in Figures 6 and 7, respectively, as solid lines. The absorption spectrum of NilPc is similar to that of tribenzotetraazaporphine without peripheral substituent groups,[20] and the spectrum of BenPc is typical of those of metal-free Pc's.[18] All compounds show the split Q_{0-0}-bands due to the low symmetry of the molecules. The splitting in NilPc (2017 cm^{-1}) is particularly large compared with those of the other four compounds. Comparison of this energy in BenPc, NapPc, and AnPc (684, 817, and 914 cm^{-1}, respectively) indicates that the larger the introduced conjugation unit, the larger will be the splitting of the Q_{0-0}-band, although the molecular symmetry is C_{2v} in each case. In PyPc, this splitting is 640 cm^{-1}, a value slightly smaller than the benzene analogue, i.e., BenPc.

The Q_{0-0} peaks shift to longer wavelength with enlargement of the π-conjugated system, while the extent of the band shift decreases with increasing molecular size. If we take the center of the two split Q_{0-0} peaks as the positions of the Q-band, then the energy differences of the Q-bands among NilPc to AnPc are 1030, 506, and 463 cm^{-1} for NilPc−BenPc, BenPc−NapPc, and NapPc−AnPc, respectively. The absorption coefficients (ϵ) of the Q-bands decrease generally with decreasing symmetry of the molecules, i.e., BenPc > NapPc > AnPc > NilPc, while the ratio of the actual absorption (the oscillator strength) at 500−800 nm (the Q-band) is 0.75:1.00:1.03:0.88 for NilPc:BenPc:NapPc:AnPc, suggesting that the Q-band does not intensify indefinitely with increasing molecular size. Small peaks seen at 454 nm for NapPc and at 462 nm for AnPc may not be ascribed to the naphthalene or anthracene moiety, since the absorption bands of naphthalene and anthracene appear generally below ca. 300 or 400 nm, respectively.[21]

The spectra of deprotonated ($-H_2$) species are shown as broken lines (Figure 6). The Q-bands of ($-H_2$)BenPc and ($-H_2$)NapPc are close to those of MtPc's with D_{4h} symmetry,[14,18] indicating that elimination of two pyrrole protons

(14) Luk'yanets, E. A. *Electronic Spectra of Phthalocyanines and Related Compounds*; NIOPIK: Moscow, 1989. Kobayashi, N. In *Phthalocyanines—Properties and Applications*; Leznoff, C. C., Lever, A. B. P., Eds.; VCH: New York, 1992; Vol. 2, Chapter 3.

(15) (a) Bloor, J. E.; Schlabits, J.; Wolden, C. C.; Demerdache, A. *Can. J. Chem.* **1964**, *42*, 2201. (b) Cuellar, E. A.; Marks, T. J. *Inorg. Chem.* **1981**, *20*, 3766. (c) Day, V. W.; Marks, T. J.; Wacher, W. A. *J. Am. Chem. Soc.* **1975**, *97*, 4519.

(16) Kobayashi, N.; Lever, A. B. P. *J. Am. Chem. Soc.* **1987**, *109*, 7433.

(17) Aoudia, M.; Cheng, G.; Kennedy, V. O.; Kenney, M. E.; Rodgers, M. A. J. *J. Am. Chem. Soc.* **1997**, *119*, 6029.

(18) Stillman, M. J.; Nyokong, T. In *Phthalocyanines—Properties and Applications*; Leznoff, C. C., Lever, A. B. P., Eds.; VCH: New York, 1989; Chapter 3.

(19) Lever, A. B. P.; Licoccia, S.; Ramaswamy, B. S. *Inorg. Chim. Acta* **1982**, *64*, L87.

(20) Elvidge, J. A.; Linstead, R. P. *J. Chem. Soc.* **1955**, 3536.

(21) Kobayashi, N.; Minato, S.; Osa, T. *Makromol. Chem.* **1983**, *184*, 2123.

Table 1. Experimental Determination of (A) the Longest Wavelength Band Parameters in Chloroform (SubAP and tBSubPc) and in *o*-Dichlorobenzene (Others) and (B) the MCD Parameters of the Q-Band

(A) Longest Wavelength Band Parameters in Chloroform and in *o*-Dichlorobenzene

compd	λ_{max}/nm (λ_{max}/kcm^{-1})	ϵ	half-width at 1/e height/cm^{-1}	dipole strength/D^2	dipole length/Å	$[\theta]_M$	$B/D \times 10^4$ [a]
SubAP[b]	411 (24.331)	12 200	3005	24.57	1.034		
tBSubPc	567 (17.637)	51 500	378	18.00	0.885		
SubNc	667 (14.993)	62 600	451	30.71	1.116		
NilPc	680 (14.706)	58 500	267.6	17.359	0.869	−24.7	21.6
BenPc	700 (14.286)	122 000	241.8	33.673	1.210	−125.6	52.7
NapPc	729 (13.717)	91 000	258.8	27.996	1.103	−80.6	45.3
AnPc	757 (13.210)	41 200	273.4	13.891	0.777	−41.4	51.4
PyPc	688 (14.535)	112 000	249.2	31.312	1.167	−144.1	65.9

(B) MCD Parameters of the Q-Band[c]

compd	UV/nm	Γ/cm^{-1}	A/D[d]	μ[e]	$[\theta]_1$	$[\theta]_2$	diff	sum	$B/D \times 10^4$ [f]
tBSubPc[g]	567	593	0.846	−1.692	−32.0	+5.3	−37.3	−26.7	17.99
SubNc[h]	667	715	0.972	−1.944	−33.1	+10.1	−43.2	−23.0	12.75

[a] *B/D* values in systems not containing transitions to the degenerate excited states. [b] The 411-nm band is tentatively assumed as the Q-band. [c] To obtain *A/D* values by Briat's method (Briat, B.; Schooley, D. A.; Records, R.; Bunnenberg, E.; Djerassi, C. *J. Am. Chem. Soc.* **1967**, *89*, 7062), $[\theta]_1$ and $[\theta]_2$ in this table are expressed by molar ellipticity per unit gauss. Γ is the width at half-maximum absorption. diff = $[\theta]_1 - [\theta]_2$, sum = $[\theta]_1 + [\theta]_2$, and $A/D = -1.97\Gamma(\text{diff})/\epsilon_m$, while $B/D = -3.47(\text{sum}/\epsilon_m)$. Faraday *A* and *B* terms are expressed by β D^2 and β D^2/cm^{-1}, respectively, as in Stephens, P. J.; Suetaak, W.; Schatz, P. N. *J. Chem. Phys.* **1966**, *44*, 4592. [d] *A/D* values under a new definition (Piepho, S. B.; Schatz, P. N. *Group Theory in Spectroscopy*; John Wiley & Sons: New York, Chichester, 1983) are obtained by dividing these values by 2. [e] Magnetic moment. [f] *B/D* values associated with *A* terms. [g] In chloroform. [h] In *o*-dichlorobenzene.

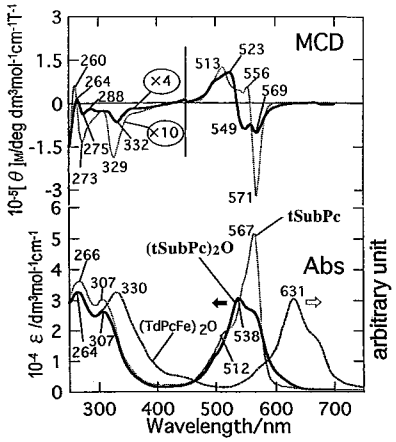

Figure 5. MCD (top) and electronic absorption spectra (bottom) of tBSubPc (• • •) and (tBSubPc)$_2$O (—) in $CHCl_3$. The electronic spectrum of μ-oxobis{tetra(dodecylsulfonamide)phthalocyaninatoiron(III)},(TdPcFe)$_2$O, in DMF (bottom, - - -) is replotted for comparison from ref 19.

helps lessen the difference between the Q_x- and Q_y-bands. This is also reflected in the spectra of (−H$_2$)NilPc and (−H$_2$)AnPc. Differing from the case of (−H$_2$)BenPc, however, (−H$_2$)PyPc still shows two Q_{0-0}-band (a peak and a shoulder), suggesting that replacement of the benzene ring with a pyridine ring further lowers the molecular symmetry. There is one common spectroscopic change in the Soret band region on deprotonation: the relatively sharp Soret bands in NilPc to PyPc become weaker and extend to longer wavelengths. Thus, in general, at least three bands are seen between 300 and 500 nm.

The MCD spectra of porphyrins with C_{2v} symmetry can be interpreted as a superimposition of Faraday *B* terms.[18] MCD spectra of neutral NilPc to PyPc (Figure 7, solid lines) can also be interpreted as a superimposition of Faraday *B* terms. For

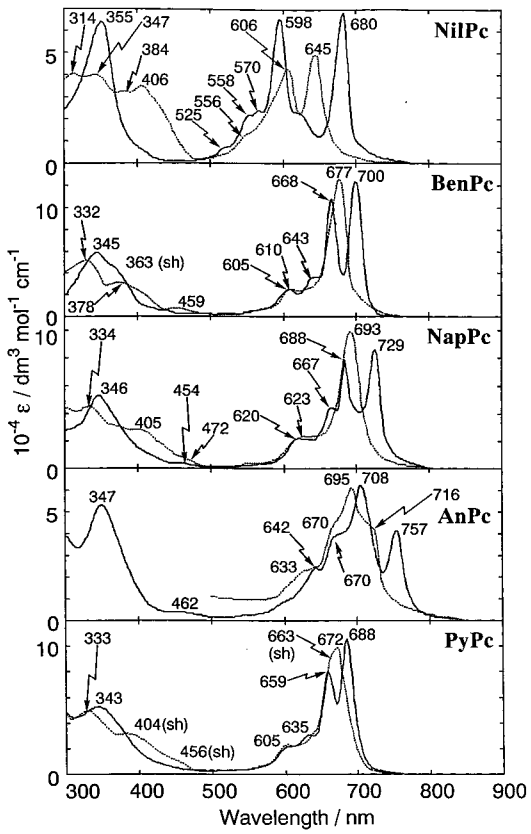

Figure 6. UV−visible−near-IR absorption spectra of NilPc−PyPc (top to bottom) in *o*-dichlorobenzene. (—) Neutral forms; (- - -) deprotonated forms obtained by addition of tetrabutylammonium hydroxide. Because of solution instability, a well-defined curve was not obtained in the Soret region of deprotonated AnPc.

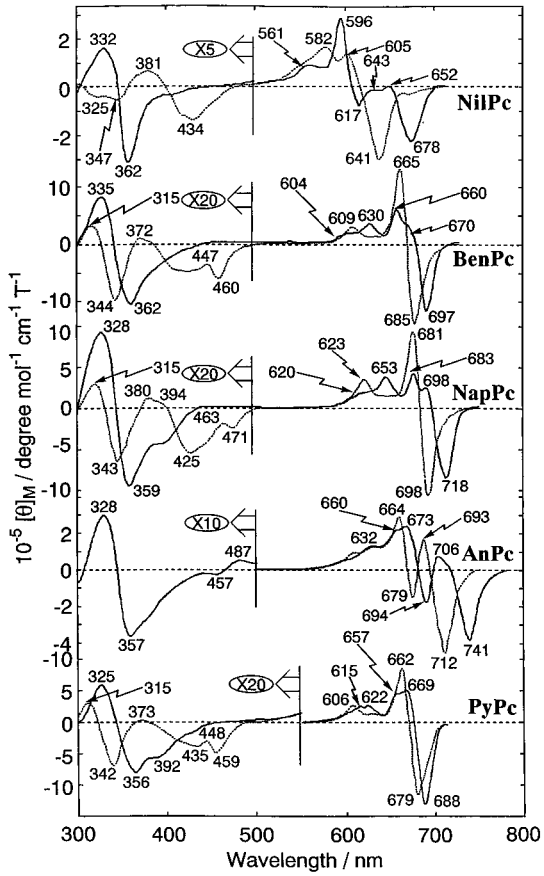

Figure 7. MCD spectra of NilPc−PyPc (top to bottom) in *o*-dichlorobenzene. (—) Neutral species; (- - -) deprotonated species obtained by addition of tetrabutylammonium hydroxide. Because of solution instability, a well-defined curve was not recorded in the Soret region of deprotonated AnPc.

example, in NilPc, the Q-band MCD maximum and minimum appear corresponding to the two intense Q peaks, and the shape of the Q-band MCD of BenPc and PyPc resembles that of metal-free Pc's with D_{2h} symmetry. The Soret band MCD spectra of NilPc to PyPc are, on the other hand, relatively simple, showing a strong dispersion type curve corresponding to the main Soret absorption peaks. Although these look like Faraday *A* terms, they are being caused by the superimposition of close Faraday *B* terms,[22] since no degenerate state is expected for these molecules theoretically.[18]

When the molecule is deprotonated (Figure 7, broken lines), the Q-band MCD of ($-H_2$)BenPc and ($-H_2$)NapPc can be interpreted as a pseudo-Faraday *A* term, since a single Q_{0-0}-band is seen in the absorption spectra. In contrast, the Q-band MCD spectra of ($-H_2$)NilPc and ($-H_2$)PyPc are considered to be a contribution of Faraday *B* terms, since the minimum and maximum of MCD correspond to the two Q_{0-0} absorption peaks. In the Soret region, although several Faraday *A* term type curves are seen, the ones detected for ($-H_2$)BenPc, ($-H_2$)NapPc, and ($-H_2$)PyPc at 440−480 nm might be pseudo-Faraday *A* terms, which are often observed for MtPc's with D_{4h} symmetry (a $\pi-\pi^*$ transition from low-lying a_{2u} to the LUMO, i.e., $4a_{2u}$ to $7e_g$).[18]

(ii) Emission Spectroscopy. (a) SubAP, tBSubPc, SubNc, and SubCRPc. Fluorescence emission and excitation spectra of monomeric subazamacrocycles in this study are shown in

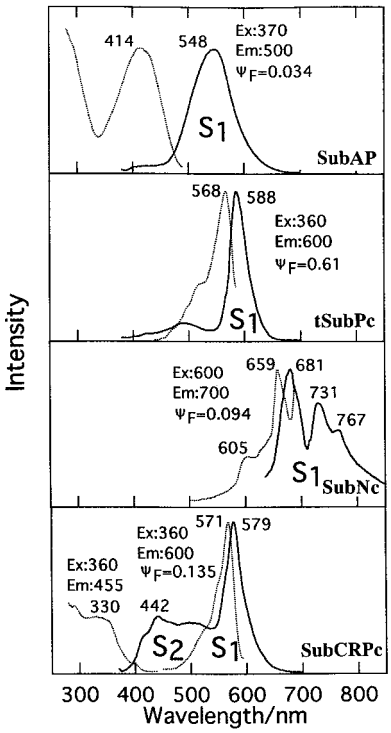

Figure 8. Fluorescence emission (solid lines) and excitation spectra (broken lines) of SubAP, tBSubPc, SubNc, and SubCRPc (top to bottom) in $CHCl_3$. Excitation wavelengths and emission wavelengths used to record excitation spectra are shown. The absorbance at the excitation wavelengths was always less than 0.05.

Figure 8. All compounds exhibit so-called S_1 emission, while only SubCRPc shows S_2 emission additionally, and they have a mirror-image relationship with respect to their excitation spectra. The S_2 emission is broader than the S_1 emission and has a band shape similar to that observed for phthalocyanine[23,24] and tetrabenzoporphyrin.[25] Interestingly, the Stokes shift for S_1 emission increases with decreasing molecular size, so that compounds showing Q-band at shorter wavelengths have larger shifts. The values of Stokes shift were 59064, 5988, 4902, and roughly ca. 400−600 cm^{-1} in the order of SubAP, tBSubPc, SubNc, and general Pc's.[24a] The value of S_1 Stokes shift of SubAP is within the size of that found for S_2 emission of Pc's (roughly 46 000−74 000 cm^{-1}).[24b] This result indicates experimentally that the spacing of the vibrational level indeed becomes smaller as the size of the π-system increases.

By using the known quantum yields of quinine sulfate (for SubAP), tetraphenylporphyrin (for tBSubPc), Rhodamine B (for SubCRPc), and compound PyPc (for SubNc) as calibrants,[26] the quantum yields (ϕ_F) of S_1 emission for SubAP, tBSubPc, SubCRPc, and SubNc were determined to be 0.034, 0.61, 0.135 (in chloroform), and 0.094 (in *o*-dichlorobenzene), respectively. The value for tBSubPc is smaller than that for tBH_2Pc (0.85)[27a] but slightly larger than that for *tert*-butylated metal-free tetra-

(22) Tajiri, A.; Winkler, J. *Z. Naturforsch.* **1983**, *38a*, 1263. Kaito, A.; Nozawa, T.; Yamamoto, T.; Hatano, M.; Orii, Y. *Chem. Phys. Lett.* **1977**, *52*, 154.

(23) Kobayashi, N.; Lam, H.; Nevin, W. A.; Janda, P.; Leznoff, C. C.; Koyama, T.; Monden, A.; Shirai, H. *J. Am. Chem. Soc.* **1994**, *116*, 879.

(24) (a) Kobayashi, N.; Togashi, M.; Osa, T.; Ishii, K.; Yamauchi, S.; Hino, H. *J. Am. Chem. Soc.* **1996**, *118*, 1073. (b) Kaneko, Y.; Nishimura, Y.; Takane, N.; Arai, T.; Sakuragi, H.; Kobayashi, N.; Matsunaga, D.; Pac, C.; Tokumaru, K. *J. Photochem. Photobiol. A: Chem.* **1997**, *106*, 177.

(25) Bajema, L.; Gouterman, M. *J. Mol. Spectrosc.* **1971**, *39*, 421. Fielding, P. E.; Mau, A. W.-H. *Aust. J. Chem.* **1976**, *29*, 933. Aaviksoo, J.; Freiberg, A.; Savikhin, S.; Stehlmakh, G. F.; Tsvirko, M. P. *Chem. Phys. Lett.* **1984**, *111*, 275.

(26) (a) Demas, J. N.; Crosby, G. A. *J. Phys. Chem.* **1971**, *75*, 991. (b) Seybold, P. G.; Gouterman, M. *J. Mol. Spectrosc.* **1969**, *31*, 1. (c) Strickler, S. J.; Berg, R. A. *J. Chem. Phys.* **1962**, *37*, 814.

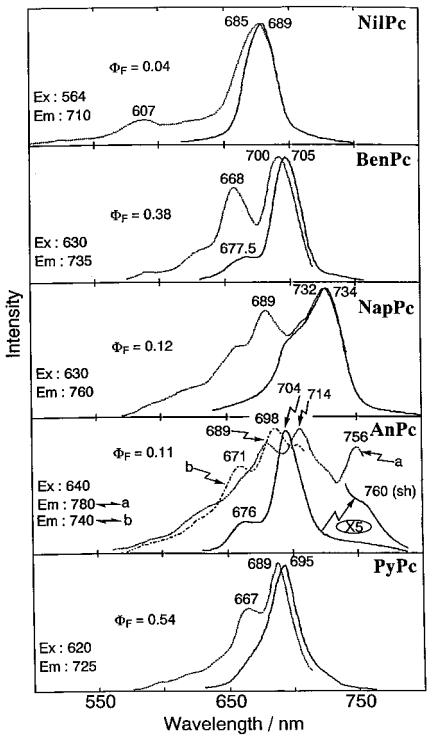

Figure 9. Fluorescence emission (—) and excitation spectra (- - -) of NilPc−PyPc (top to bottom) in *o*-dichlorobenzene. Excitation wavelengths and emission wavelengths used to record excitation spectra are shown. The absorbance at the excitation wavelengths was always less than 0.05.

benzoporphyrin (0.57) in the same solvent.[27b] The value of 0.094 for SubNc is also smaller than that for tBH_2Nc (0.14).[27a] The small value of 0.034 for SubAP may be related to the presence of both CN and CF_3-phenyl group in this molecule; i.e. the presence of two polar molecules may lead to the occurrence of intramolecular charge transfer.

(b) Ring-Expanded Low-Symmetrical Pc Analogues. Figure 9 shows the fluorescence and excitation spectra of NilPc−PyPc. Consistent with the absorption spectra, the main peak of the emission generally shifts to longer wavelengths with the enlargement of π-macrocycles, with the exception of compound AnPc, which gave a peak at shorter wavelength than expected. However, even in the case of AnPc, weak emission is seen at ca. 760 nm as a shoulder corresponding to the Q-band to the longest wavelength. The Stokes shifts are very small in each case. In general, transitions involving emission in a condensed organic molecule always takes place from the lowest excited electronic level independently of the order of levels to which the molecules was excited upon absorption of light.[28] This feature is typically seen for NilPc, where the intense fluorescence band at 689 nm coincides with the first absorption band $Q_{x(0-0)}$, which is assumed to correspond to the first excited electronic level.

The values of quantum yields (ϕ_F) are also given in the figure. The value for BenPc ($\phi_F = 0.38$) is almost 60% of that for metal-free Pc in the same solvent ($\phi_F = 0.60$),[26b] and the values for NilPc, NapPc, and AnPc are much smaller, indicating that lowering of molecular symmetry greatly destabilizes the S_1 state.[24a,29] One possible cause for this may be the difference of vibrational mode between Pc analogues with D_{2h} or D_{4h} symmetry and C_{2v} symmetry. It is noteworthy that the ϕ_F value for PyPc (0.54) is higher than that for AnPc (0.38).

Table 2. S_1 Quantum Yields (ϕ_F) and Lifetimes (τ) in Deaerated Chloroform at Room Temperature[a]

compd	ϕ_F	τ/ns	compd	ϕ_F	τ/ns
SubAP	0.03	2.51	NilPc	0.04	4.61
tBSubPc	0.61	2.10	BenPc	0.38	7.68
SubCRPc	0.14	1.35	NapPc	0.12	6.53
SubNc	0.09	1.93	AnPc	0.11	6.19
			PyPc	0.54	7.77

[a] Data on SubNc alone were collected in *o*-dichlorobenzene due to its low solubility in chloroform.

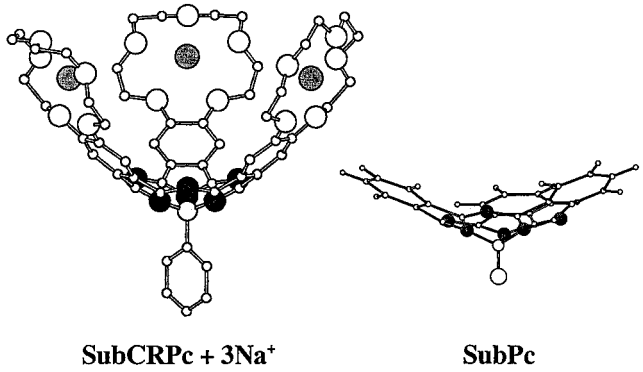

Figure 10. Structure of SubCRPc optimized using the UNIVERSAL 1.02 force field,[52] which was implemented in Program Package Cerius2. Hydrogens are omitted for clarity, and three Na^+ ions are trapped in the 15-crown-5 moiety. Oxygen and boron atoms are represented by large open circles, while nitrogens are by solid circles. The structure of SubPc with a Cl axial ligand is also shown for comparison from ref 6b. Attachment of crown ether units further deforms the π-structure of SubPc.

The quantum yields and lifetimes of all compounds in this study are summarized in Table 2. The lifetimes of subazamacrocycles are less than half of those of compounds NilPc−PyPc, indicating that they are generally smaller for compounds having smaller quantum yields.

III. Effect of Extraneous Cations. In the case of tetra-[16,30] or tricrowned[24a] Pc's (MtCRPc's), addition of some cations induces dimerization. Since we succeeded in preparing SubCRPc, we examined whether it can be dimerized by the addition of some cations. As in the previous MtCRPc system, SubCRPc was first dissolved in chloroform, and then concentrated solutions of CH_3COOK, CH_3COOCs, CH_3COORb, or CH_3COONa dissolved in chloroform−methanol (9:1 v/v) were added under stirring using a microsyringe, while the accompanying absorption spectroscopic changes were monitored. However, in no case did we find any appreciable change. In the case of MtCRPc, a hypsochromic shift accompanying a hypochromic effect on the Q-band was the indication of cofacial dimerization, and this was attained when cations which form 1:2 complexes with 15-crown-5, such as K^+, Cs^+, and Rb^+, were added. From the absence of this kind of change, we conjecture that the cone-shaped structure of SubPc[6b] prevents dimerization. The most probable structure obtained by a force field calculation (Figure 10) suggests that three crown ether units deviate so severely from planarity, forming a wine glass

(27) (a) Kobayashi, N.; Higashi, Y.; Osa, T. *Chem. Lett.* **1994**, 1813. (b) Kobayashi, N.; Numao, M.; Kondo. R.; Nakajima, S.; Osa, T. *Inorg. Chem.* **1991**, *30*, 2241.

(28) Kasha, M. *Discuss. Faraday Soc.* **1950**, *9*, 14.

(29) Kobayashi, N.; Ashida, T.; Osa, T. *Chem. Lett.* **1992**, 1567, 2031. Kobayashi, N.; Ashida, T.; Osa, T.; Konami, H. *Inorg. Chem.* **1994**, *33*, 1735.

(30) Koray, A. R.; Ahsen, V.; Bekaroglu, O. *J. Chem. Soc., Chem. Commun.* **1986**, 932. Sielcken, O. E.; van Tiborg, M. M.; Roks, M. F.; Hendricks, R.; Drenth, W.; Nolte, R. J. M. *J. Am. Chem. Soc.* **1987**, *109*, 4261.

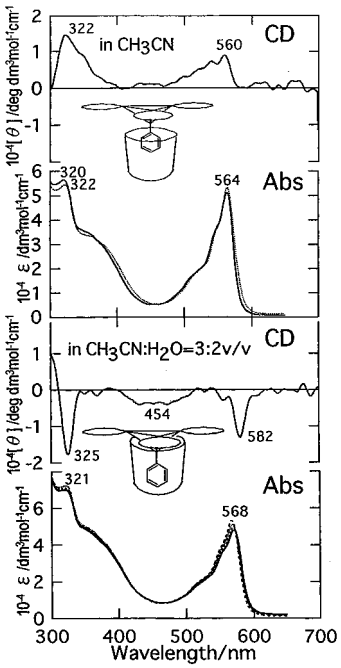

Figure 11. Electronic absorption and ICD spectra of SubCRPc in the absence (···) and presence (—) of DMβCD in CH_3CN (top) and in CH_3CN-H_2O (3:2 v/v) mixture (bottom). [DMβCD]/M = 6.59×10^{-3}. Absorption spectra drawn with other lines are those obtained at lower [DMβCD].

structure, that it is impossible to form a cofacial dimer on the addition of cations.

IV. Host−Guest Complexation with 2,6-Dimethyl-β-Cyclodextrin. Since SubCRPc contains a phenyl group as an axial ligand, its complexation with cyclodextrins (CDxs) was studied using electronic absorption and circular dichroism spectroscopy. As a CDx, 2,6-dimethyl-β-cyclodextrin (DMβCDx) was chosen from size and solubility considerations.[31] The results in two systems, acetonitrile and acetonitrile−water (3:2 v/v) mixtures, are shown in Figure 11. The addition of DMβCDx to a solution containing SubCRPc results in a small change in the absorption spectra, suggesting interaction between SubCRPc and DMβCDx. Inclusion of the crown moiety of the SubPc molecule is impossible since its size is much larger than that of the CDx cavity. Although inclusion of the phenyl moiety seems natural, ^{1}H NMR measurements were performed in the presence and absence of DMβCDx in order to confirm this. In the absence of DMβCDx, the signals of *ortho*, *meta*, and *para* protons of the phenyl group appeared at 5.400, 6.641, and 6.763 ppm, respectively. With increasing DMβCDx concentration, all signals shifted to upper field;[32] for example, at [DMβCDx] = 3.3×10^{-3} mol/L, the shifts were 0.013, 0.198, and 0.115 ppm for *ortho*, *meta*, and *para* protons, respectively, in pure acetonitrile, while in acetonitrile−water (3:2 v/v) mixture these were 0.014, 0.203, and 0.118 ppm, respectively. Since the size of the shift reflects the magnitude of interaction between the inner wall of the DMβCDx and guest molecules, the above NMR result suggests strongly the inclusion of the phenyl moiety of SubCRPc. The 1:1 complex formation was confirmed using Job's continuous variation method[33] (not shown), and therefore the formation constant was determined to be 516 mol^{-1} L in acetonitrile−water (3:2 v/v) by the method of Rose and Drago.[34]

The induced circular dichroism (ICD) spectra in Figure 11 are, however, different in the two solvent systems. Although ICD spectra are seen corresponding to the absorption spectra of SubCRPc, their sign is opposite: mainly plus in acetonitrile and minus in the acetonitrile−water mixture. This difference may be interpreted on the basis of hitherto accumulated knowledge on the ICD of CDx−aromatic guest inclusion complexes[35] as the difference of the depth of the phenyl group in the CDx cavity as follows. It has been established both experimentally and theoretically that *electronic transitions parallel to the molecular axis of CDxs produce positive ICD, while those normal to the axis show negative ICD.*[31,35] Accordingly, the inclusion structure in acetonitrile−water (3:2 v/v) mixture can be inferred to be of the lid type,[35b] in which the macrocyclic plane of SubCRPc lies on the rim of DMβCDx. The inclusion structure in acetonitrile seems similar but is an exception of the above rule. This happens when the aromatic guest molecules lie above the rim of the CDx by more than ca. 0.3 Å along the CDx axis,[35c] and an inverse relationship with respect to the sign of circular dichroism comes into force. Thus, in acetonitrile, the phenyl group appears to be at the entrance of the CDx cavity, while in solvents containing water it would be trapped deep within the cavity. A Corey−Pauling−Koltun molecular model suggests that more than 90% of the phenyl group is trapped within the cavity in water. The driving force for the inclusion of guest molecules by CDx is the hydrophobic interaction.[31] Accordingly, in solvents containing water, hydrophobic aromatic guest molecules try to escape deep into the hydrophobic CDx cavity, while in more hydrophobic organic solvents, this kind of driving force will diminish.

V. Molecular Orbital Calculations. To deepen our understanding of the electronic absorption spectra of subazamacrocycles and their ring-expanded unsymmetrical phthalocyanine analogues, molecular orbital calculations were performed for both neutral protonated species (metal-free Pc derivatives) and pyrrole proton deprotonated dianion species (subazamacrocycles) within the framework of the Pariser−Parr−Pople (PPP) approximation.[36]Although SubPc's are not flat and have threefold rotation,[6b] π-electron calculations were adopted, since the electronic spectra of buckled SPc's have been successfully explained using MO calculations at the PPP LCAO SCF CI level of approximation.[37]

(i) SubAP, SubPc, and SubNc Structures. Some frontier MOs and MO levels of dianions of SubAP, SubPc, and SubNc (i.e., $SubAP^{2-}$, $SubPc^{2-}$, and $SubNc^{2-}$, respectively) obtained from our calculations are shown in Figures 12 and 13, respectively, with the results of calculations summarized in Table 3. The π-character in these frontier orbital is high. For example, in $SubPc^{2-}$, the π-character of the HOMO − 1, HOMO, and LUMOs are 83.3, 80.3, and 80.0%, respectively, indicating that the treatment by π-electron approximation is possible. Under C_{3v} symmetry, many transitions are doubly degenerate, since several orbitals including LUMOs are orbitally doubly degenerate. The LUMO and LUMO + 1 are degenerate for all compounds, and for SubPc and SubNc the LUMO + 2 and LUMO + 3 are doubly degenerate. Of these, the latter two

(31) *Cyclodextrins—Fundamentals and Applications*; Toda, F., Ueno, A. Eds.; Sangyo-Tosho: Tokyo, 1995.
(32) NMR signals of aromatic molecules shift to upper field in the cavity of CDxs: Wood, D. J.; Hruska, F. E.; Saenger, W. *J. Am. Chem. Soc.* **1977**, *99*, 9, 1735.
(33) Job, P. *Ann. Chim. Phys.* **1928**, *9*, 113.
(34) Rose, N. J.; Drago, R. S. *J. Am. Chem. Soc.* **1959**, *81*, 6138.
(35) (a) Kobayashi, N.; Osa, T. *Bull. Chem. Soc. Jpn.* **1991**, *64*, 1878. (b) Kobayashi, N. *J. Chem. Soc., Chem. Commun.* **1988**, 918. (c) Kobayashi, N. In ref 31; Chapter 2, Section 6.
(36) Pariser, R.; Parr, R. G. *J. Chem. Phys.* **1953**, *21*, 466, 767. Pople, J. A. *Trans. Faraday Soc.* **1953**, *46*, 1375.
(37) Marks, T. J.; Stojakovic, D. R. *J. Am. Chem. Soc.* **1978**, *100*, 1695.

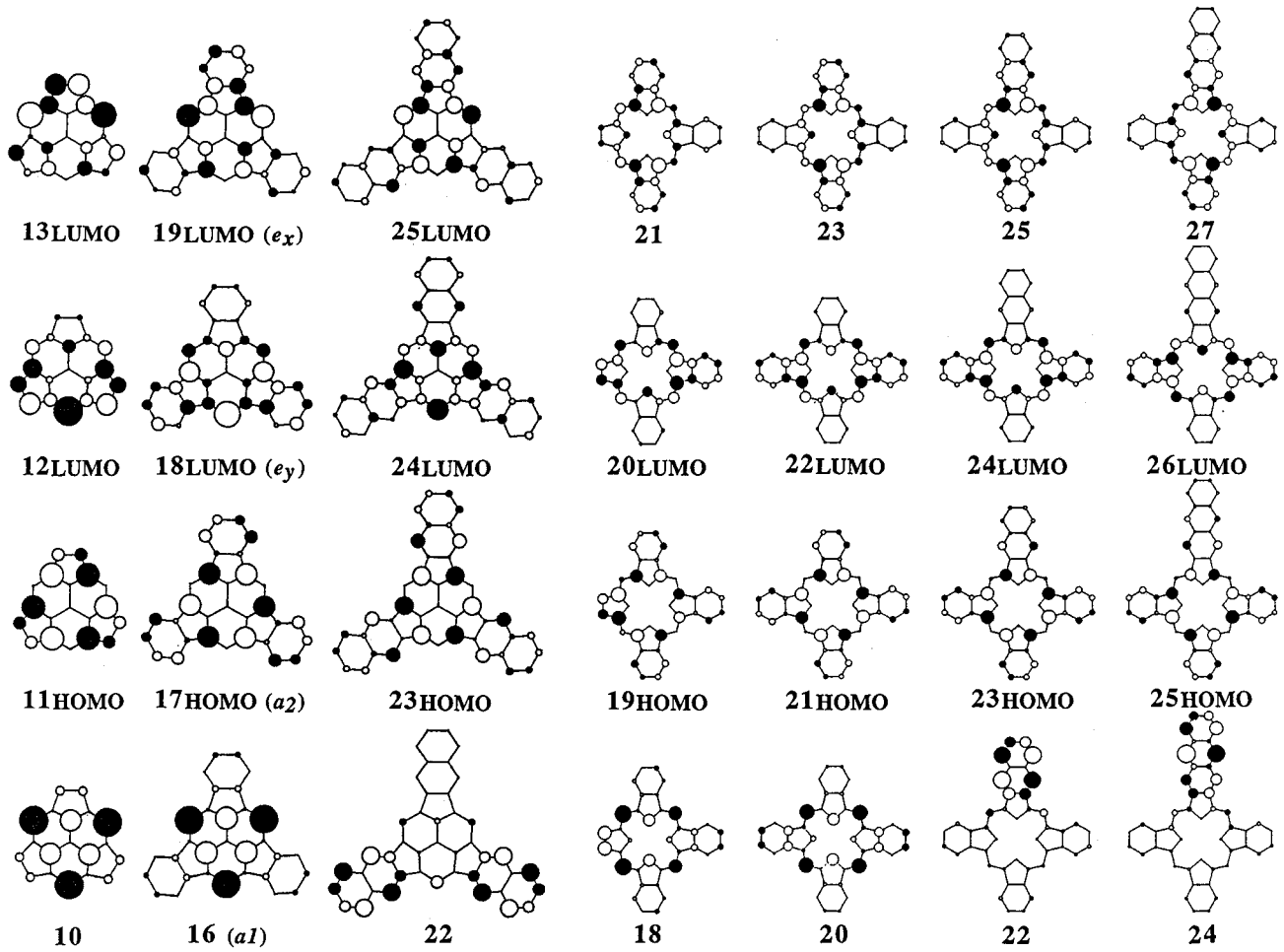

Figure 12. Four frontier orbitals of $SubAP^{2-}$, $SubPc^{2-}$, $SubNc^{2-}$, NilPc, BenPc, NapPc, and AnPc.

have larger coefficients in the outer benzene and naphthalene moieties; i.e., these are benzene- and naphthalene-centered orbitals. In addition, in the case of $SubNc^{2-}$, the HOMO − 1 and HOMO − 2 (naphthalene-centered orbitals) are also doubly degenerate. As in the experiments, the calculated Q-bands and Soret bands shift to a longer wavelength and the oscillator strength increases with increasing area of the π-systems (for example, the Q-bands of $SubAP^{2-}$, $SubPc^{2-}$, and $SubNc^{2-}$ are estimated at 468 (f = 0.06), 502 (0.56), and 540 (0.91) nm, respectively). The red-shift of the Q-band is largely explained by destabilization of the HOMOs, rather than that of the LUMOs (Figure 13), as in tetracyclic TAP, Pc, and Nc systems. The Q-band of SubAP is much weaker than that of SubPc, and this is reflected particularly in the size of the MCD magnitude (see the magnification factor, Figure 4). Although the correspondence between experiment and calculation is not particularly good for SubAP, the spectra of SubPc are reproduced well in the calculations. In particular, two strong absorption peaks in the Soret region are predicted at 322 and 268 nm for the experimental 307 and 266 nm. In addition, the calculated intensity ratio of the Soret band to the Q-band (0.89/0.56 = ca. 1.59) is close to that (roughly 1.4−1.6) in the experiments. A *z*-polarized transition was found at 286 nm (configurations 13→19(24%), 12→18(24%), 15→18(17%), 14→19(17%)); however, its strength (f = 0.009) is much less than those of the neighboring transitions. The calculated intensity of the Q-band (f = 0.56) is smaller than that of Pc^{2-} (f = 0.84), as is observed experimentally. In addition, the predicted Q-band position (502 nm) is at shorter wavelength than that of Pc^{2-} (662 nm). In the case of SubNc, the Soret region appears to be a superimposition of several transitions, and no transitions were predicted between the Soret and Q-bands, although two tiny peaks are seen at ca. 404 and 475 nm (Figure 4). As in general tetracyclic TAP, Pc, and Nc systems,[38] the "purity" of the HOMO−LUMO transition for the Q-band increases with increasing molecular size, as suggested from their configuration: 57, 84, and 89% for $SubAP^{2-}$, $SubPc^{2-}$, and $SubNc^{2-}$, respectively. However, the Soret band region is not described by a one-electron description: many transitions contribute to a comparable degree, as in the case in Pc's. Thus, from the viewpoint of MO calculations, it may be concluded that the properties of the Q-bands and Soret bands are close to those of the corresponding tetracyclic compounds (i.e., Pc and Nc). If this is the case, then the main framework of the subazamacrocyclic chromophore may be the innermost 12-membered rings containing six nitrogen atoms and carrying 14 electrons.

(ii) Compounds NilPc−AnPc. (a) Metal-Free Species. When unsymmetrical Pc and Nc analogues are prepared by the ring expansion of SubPc's and SubNc's, they are obtained as metal-free species. In contrast to the cases of normal Pc's and Nc's, which have approximate square structures, however, two cases have to be considered on the position of two pyrrole hydrogens; i.e., they can be linked to two pyrrole nitrogens either along the short or long axes of the molecule. Accordingly, MO calculations have been performed for these two cases, giving information which appears useful in interpreting the experimental spectra. The main results are summarized as follows (see

(38) Kobayashi, N.; Konami, H. In *Phthalocyanines—Properties and Applications*; Leznoff, C. C., Lever, A. B. P., Eds.; VCH: New York, 1996; Vol. 4, Chapter 9, and references therein.

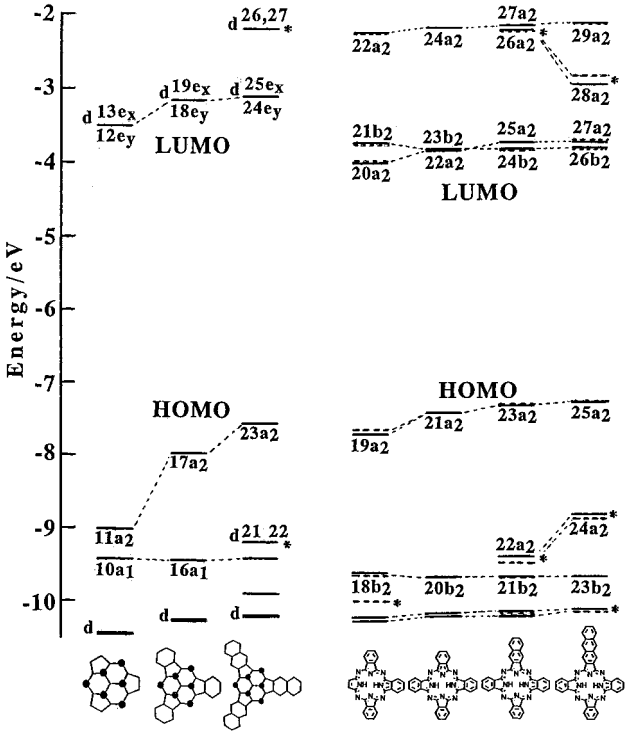

Figure 13. Partial molecular orbital energy diagram for $SubAP^{2-}$, $SubPc^{2-}$, $SubNc^{2-}$, NilPc, BenPc, NapPc, and AnPc. In the data of NilPc−AnPc, solid and broken lines indicate the data when two pyrrole protons are linked at pyrrole nitrogens along the short and long axes, respectively.

also Table 4 and Figures 12 and 13). (1) The Q-band splits into two, but the splitting is larger when the two protons are attached along the short axis. Values are 1385 (612−685 nm), 699 (664−697 nm), 775 (677−715 nm), and 891 cm^{-1} (682−726 nm) for the π-structures of NilPc, BenPc, NapPc, and AnPc, respectively, while the corresponding values are 274 (650−662 nm), 699 (664−697 nm), 356 (691−708 nm), and only 27 cm^{-1} (708−710 nm) when protons are attached along the long axis. Experimentally, the values of the Q_{0-0}-band splitting are 2017 (598−680 nm), 684 (668−700 nm), 1253 (668−729 nm), and 905 cm^{-1} (708−757 nm) for the above order, strongly suggesting that two protons are bound to the nitrogens along the short axis. (2) When the protons are along the short axis of the split Q-band, the relative intensity of the lower-energy split band becomes weaker than that at higher energy with increasing molecular size; i.e., the ratios of *f* (lower energy/higher energy) are 1.03:0.92:0.84:0.73 for NilPc:BenPc:NapPc:AnPc. There is no such regularity if protons are along the long axis; i.e., 0.83: 0.92:1.01:0.91 for NilPc:BenPc:NapPc:AnPc. (3) The intensity of the Q-band (the sum of the two calculated oscillator strengths, *f*) is similar whether the two protons are linked to two nitrogens along the short or long axis, although it *per se* increases with increasing molecular size. That is, they are 1.45 ± 0.03, 1.82, 2.01 or 2.02, 2.12 ± 0.04 in order of NilPc to AnPc, respectively. (4) The Q-band energy, defined as the energy midway between the split Q-bands, shifts to longer wavelength with increasing molecular size of the fused aromatics, but the extent of the shift becomes smaller as the macrocyclic ligand becomes larger. The calculated wavelengths are 646, 680, 695, and 703 nm when protons are attached along the short axis and 656, 681, 684, and 709 nm when they are attached along the long axis, while experimentally they are 636, 684, 697, and 731 nm in the order of NilPc to AnPc, respectively. (5) For

Table 3. Calculated Transition Energies, Oscillator Strength (*f*), and Configurations for the Dianions of Subazamacrocycles[a]

energy/eV	(nm)	*f*	configurations[b]		
			$SubAP^{2-}$		
2.6483	(468)	0.06	11→12(57%)	10→13(38%)	
2.6514	(468)	0.06	11→13(57%)	10→12(38%)	
3.4229	(362)	0.17	7→13(37%)	8→13(31%)	11→12(17%)
3.4417	(360)	0.18	7→2(38%)	11→13(18%)	9→13(18%)
			8→12(17%)		
4.1290	(300)	1.04	10→13(40%)	9→12(21%)	8→13(18%)
			11→12(16%)		
4.1438	(299)	1.00	10→12(37%)	9→13(23%)	8→12(21%)
			11→13(15%)		
4.4566	(278)	0.73	7→13(58%)	10→13(12%)	9→12(11%)
			8→13(11%)		
4.4703	(277)	0.87	7→12(59%)	10→12(14%)	9→13(12%)
			$SubPc^{2-}$		
2.4680	(502)	0.56	17→18(84%)	16→19(15%)	
2.4680	(502)	0.56	17→19 84%)	16→18(15%)	
3.8525	(322)	0.89	16→18(53%)	11→18(19%)	
3.8525	(322)	0.89	16→19(53%)	11→19(19%)	
4.1422	(299)	0.21	17→21(38%)	15→18(16%)	14→19(16%)
			11→18(11%)		
4.1422	(299)	0.21	17→20(38%)	15→19(16%)	14→18(16%)
			11→19(11%)		
4.6321	(268)	1.17	11→18(38%)	16→18(18%)	
4.6321	(268)	1.17	11→19(38%)	16→19(18%)	
			$SubNc^{2-}$		
2.2949	(540)	0.91	23→24(89%)		
2.2949	(540)	0.91	23→25(89%)		
3.8170	(325)	0.82	20→24(42%)	22→24(20%)	21→25(20%)
3.8170	(325)	0.82	20→25(42%)	22→25(20%)	21→24(20%)
4.1059	(302)	0.44	20→24(28%)	22→24(23%)	21→25(23%)
4.1059	(302)	0.44	20→25(28%)	22→25(23%)	21→24(23%)
4.3964	(282)	0.22	16→25(20%)	19→24(18%)	21→28(11%)
			20→25(11%)		
4.3966	(282)	0.22	16→24(20%)	19→25(18%)	22→28(11%)
			20→24(11%)		
4.7170	(263)	0.23	19→25(33%)	18→25(19%)	17→24(19%)
			16→24(18%)		
4.7171	(263)	0.23	19→24(33%)	18→24(19%)	17→25(19%)
			16→25(18%)		
4.8324	(257)	1.08	21→28(25%)	20→27(19%)	16→25(17%)
4.8325	(257)	1.08	22→28(25%)	20→26(19%)	16→24(17%)

[a] Excited states with less than 5.0 eV and *f* greater than 0.16 are shown in addition to two weak transitions ($f = 0.06$) of $SubAP^{2-}$ at 468 nm. [b] Orbital numbers 11, 17, and 23 are HOMOs of $SubAP^{2-}$, $SubPc^{2-}$, and $SubNc^{2-}$, respectively. In $SubNc^{2-}$, the MOs numbered 21, 22 and 26, 27 are doubly degenerate naphthalene-centered orbitals.

compounds containing a naphthalene or an anthracene moiety, the HOMO − 1 and LUMO + 2 orbitals are these molecule-centered orbitals. As can be judged from the results in Table 4, naphthalene- or anthracene-centered transitions overlap mainly with the Soret band, while an anthracene-centered transition is predicted between the Q-bands and Soret bands. Consistent with this prediction, a clear peak is seen at 462 nm in the spectrum of AnPc, although its intensity is not large. (6) Two Q-bands are essentially described by a one-electron description (Table 4), but its purity increases with increasing molecular size. For example, when the two protons are along the short axis, the percentage of the HOMO to the LUMO transition of the Q-band to lower energy increases from 87% of NilPc to 88% of BenPc, and further to 89% of NapPc and AnPc. This is the same phenomenon as for (pyrrole proton) deprotonated species.[24a] Thus, almost all the data for the Q-band support the case that the two pyrrole protons are along the short axis. The features in the shorter wavelength region are very complex. (7) The split B1 bands are no longer described in a one-electron description, since they appear to be mixtures of several configurations. In

Table 4. Calculated Transition Energies, Oscillator Strength (*f*), and Configurations for Metal-Free NilPc−AnPc[a]

energy/eV	(nm)	*f*	configurations[b]			obsd (nm)	energy/eV	(nm)	*f*	configurations[b]		
NilPc (two protons along the short axis)							**NilPc** (two protons along the long axis)					
1.8553	(668)	0.72	19→20(87%)	18→21(12%)		(680)	1.8724	(662)	0.67	19→21(84%)	18→20(15%)	
2.0271	(612)	0.70	19→21(87%)	18→20(12%)		(598)	1.9064	(650)	0.81	19→20(90%)		
3.6405	(341)	2.14	18→20(77%)	19→21(12%)			3.2401	(383)	0.20	17→20(88%)		
3.7468	(331)	1.28	18→21(42%)	15→21(37%)			3.5976	(345)	1.23	14→20(42%)	18→20(33%)	
3.9274	(316)	0.21	19→23(49%)	16→21(26%)	15→20(17%)		3.8027	(326)	0.37	17→21(75%)	18→21(18%)	
4.0017	(310)	0.91	16→20(54%)	18→21(27%)	15→21(12%)		3.8744	(320)	1.78	14→20(48%)	18→20(39%)	
4.1160	(301)	0.33	14→20(65%)	15→21(12%)	17→21(11%)		3.9159	(317)	1.73	18→21(46%)	17→21(24%)	15→20(21%)
4.2072	(295)	0.17	15→20(54%)	16→21(37%)			4.1961	(295)	0.14	15→20(44%)	16→21(26%)	18→21(18%)
4.2721	(290)	0.15	16→20(34%)	15→21(29%)	17→21(15%)		4.1961	(275)	0.16	14→21(93%)		
4.3723	(284)	0.17	17→21(57%)	19→25(14%)	14→20(12%)		4.5033					
BenPc							**BenPc**					
1.7797	(697)	0.87	21→22(88%)	20→23(12%)		(700)	1.7797	(697)	0.87	21→22(88%)	20→23(12%)	
1.8664	(664)	0.95	21→23(91%)			(668)	1.8664	(664)	0.95	21→23(91%)		
3.6563	(339)	1.40	20→23(47%)	17→23(43%)			3.6563	(339)	1.40	20→23(47%)	17→23(43%)	
3.8200	(325)	1.96	20→22(68%)	21→26(14%)			3.8200	(325)	1.96	20→22(68%)	21→26(14%)	
3.9696	(312)	0.23	21→26(85%)				3.9696	(312)	0.23	21→26(85%)		
4.0317	(308)	1.62	17→23(51%)				4.0317	(308)	1.62	17→23(51%)		
4.2268	(293)	0.17	21→27(89%)				4.2268	(293)	0.17	21→27(89%)		
4.2678	(291)	0.37	17→22(91%)				4.2678	(291)	0.37	17→22(91%)		
NapPc (two protons along the short axis)							**NapPc** (two protons along the long axis)					
1.7350	(715)	0.92	23→24(89%)	21→25(10%)		(729)	1.7520	(708)	1.01	23→25(88%)	21→24(10%)	
1.8311	(677)	1.10	23→25(91%)			(688)	1.7930	(691)	1.00	23→24(92%)		
3.5336	(351)	1.15	22→25(66%)	21→24(24%)			3.5409	(350)	1.78	21→24(39%)	22→25(34%)	18→24(16%)
3.6890	(336)	0.19	22→24(64%)	21→25(14%)	23→28(11%)		3.8899	(319)	1.82	21→25(72%)		
3.7283	(333)	1.42	21→25(40%)	20→25(24%)	22→24(20%)		4.0122	(309)	1.22	18→24(36%)	21→24(31%)	23→29(15%)
3.8566	(321)	0.43	23→29(60%)	21→24(19%)	22→25(15%)		4.1644	(298)	0.29	23→29(67%)	20→24(15%)	
3.9523	(314)	0.64	23→29(38%)	21→24(34%)	22→25(11%)		4.3435	(285)	0.22	18→25(82%)		
3.9730	(312)	0.69	20→25(63%)	21→25(14%)	18→25(14%)		4.5808	(271)	0.50	22→26(60%)	16→24(21%)	
4.1714	(297)	0.22	18→25(55%)	23→30(29%)								
4.1889	(296)	0.20	20→24(62%)	17→24(19%)								
4.1993	(295)	0.24	23→30(63%)	19→24(15%)	18→25(11%)							
4.6505	(267)	0.38	22→26(45%)	16→24(42%)								
AnPc (two protons along the short axis)							**AnPc** (two protons along the long axis)					
1.7079	(726)	0.91	25→26(89%)			(757)	1.7468	(710)	0.99	25→27(93%)		
1.8184	(682)	1.24	25→27(92%)			(708)	1.7501	(708)	1.09	25→26(89%)		
3.1889	(389)	0.35	24→27(73%)				3.2640	(380)	0.90	24→27(72%)	23→26(11%)	
3.6986	(335)	0.21	24→28(46%)	23→27(29%)	22→27(11%)		3.6408	(341)	0.80	20→26(44%)	23→26(36%)	24→27(11%)
3.7826	(328)	1.68	24→28(36%)	23→27(23%)	21→27(21%)		3.9213	(316)	2.18	23→27(55%)		
3.7868	(327)	1.95	23→26(56%)	25→31(23%)			3.9681	(312)	1.50	20→26(43%)	23→26(33%)	25→32(11%)
3.8942	(318)	0.50	25→31(74%)	23→26(15%)			4.1407	(299)	0.17	22→26(61%)	25→32(25%)	
4.0005	(310)	1.02	22→27(60%)	23→27(19%)			4.3671	(284)	0.35	20→27(73%)	22→27(11%)	
4.1266	(300)	0.24	22→26(56%)	19→26(27%)								
4.2327	(293)	0.15	21→26(61%)	19→27(21%)								
4.3832	(283)	0.30	20→27(50%)	21→26(19%)								

[a] Excited states with less than 5.0 eV and *f* greater than 0.14 are shown. [b] Orbital numbers 19, 21, 23, and 25 are HOMOs of NilPc, BenPc, NapPc, and AnPc, respectively. In NapPc, the MOs numbered 22 (HOMO − 1) and 26 (LUMO + 2) are naphthalene-centered orbitals. Similarly, in AnPc, MOs 24 (HOMO − 1) and 28 (LUMO + 2) are anthracene-centered orbitals.

particular, the naphthalene- or anthracene-centered transition is mixed significantly in NapPc and AnPc, respectively.

(b) Deprotonated (−H_2) Species. As in experiment (Figures 6 and 7, dotted lines), the calculated splitting of the Q-band decreases on deprotonation, i.e., 526 (622−643 nm), 0 (662−662 nm), 179 (673−681 nm), and 359 (676−693 nm) cm^{-1} for (−H_2)NilPc, (−H_2)BenPc, (−H_2)NapPc, and (−H_2)AnPc, respectively. The orders of magnitude of the experimental values for (−H_2)NilPc (998 cm^{-1}), (−H_2)BenPc and (−H_2)NapPc (0 cm^{-1}), and (−H_2)AnPc (422 cm^{-1}) agree with the above calculation trend. In addition, as shown particularly for (−H_2)-NilPc in Figure 6, the sum of the intensity of the two Q transitions may be smaller for deprotonated species. Changes in the Soret region are difficult to extract.

The energy levels of frontier orbitals are not compared in Figure 13 because of the complexity of the lines. However, the situation is very similar to that of metal-free derivatives, except that some orbitals become doubly degenerate. In (−H_2)NapPc and (−H_2)AnPc, naphthalene- or anthracene-centered orbitals appear at approximately the same positions as in NapPc and AnPc. In general, the HOMOs destabilize more than the LUMOs with increasing size of the π-systems, both in the subazamacrocycles and unsymmetrical Pc analogues.

(iii) Origin of the Reactivity of SubPc for the Ring Expansion. We may guess intuitively that the high reactivity of SubPc for the ring expansion reaction is related to its cone-shaped distorted structure. Accordingly, we first calculated the bond energies in SubPc and, for comparison, MgPc using density functional theory (DFT)/natural bond orbital (NBO) treatment[39] in the *ab initio* MO program package Gaussian94/DFT.[40] The calculated bond energies for the C−N bonds are summarized in Table 5. The numbers in the table show little deviation (0.4−0.5 kJ/mol per N−C bond) between the two compounds, suggesting that the distortion energy is not a major cause of the ring expansion reactivity. We then investigated the reactivity

Table 5. Bond Energies[a] for the C−N Bond of the Innermost 12-Membered (SubPc) and 16-Membered (MgPc) Rings

	SubPc			MgPc		
bond	σ	π	total	σ	π	total
N(pyrrole)−αC	−0.81481	−0.34587	−1.16068	−0.82708	−0.31720	−1.14428
N(meso)−αC	−0.87521	−0.33179	−1.20700	−0.87290	−0.31230	−1.18520

[a] In kcal/mol.

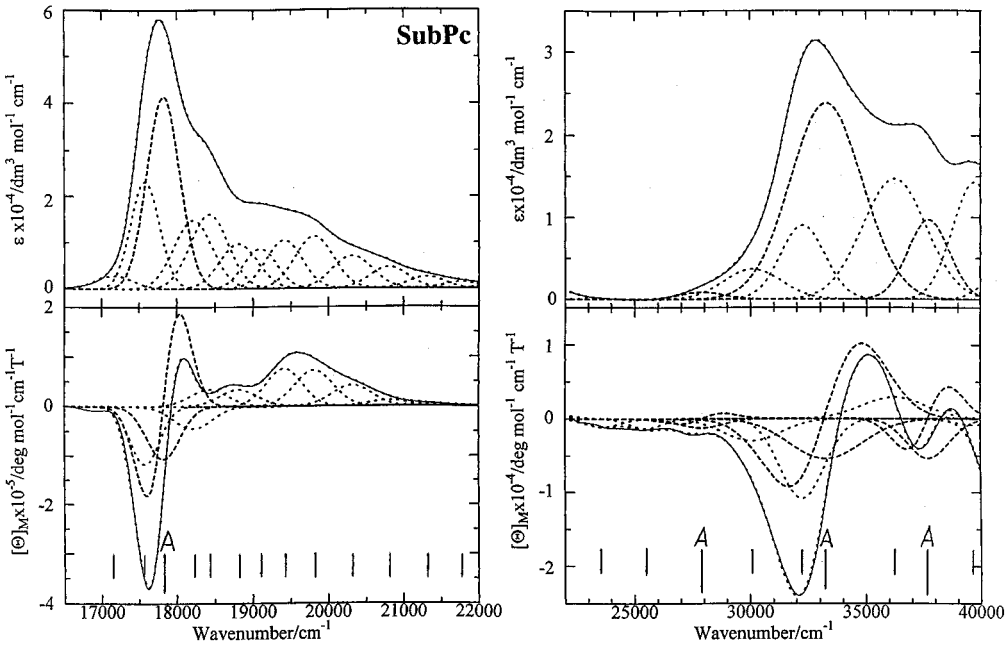

Figure 14. Electronic absorption (top) and MCD (bottom) band analysis for SubPc with a Cl axial ligand in $CHCl_3$. Experimental data are plotted by solid lines, while individual *B* term type bands and fitted data are by dotted lines. *A* term type bands and associated *B* term bands are drawn by broken lines. The vertical lines show the band center positions (long lines are *A* terms).

of SubPc from the viewpoint of ligation energy of the pyrrole nitrogen atoms to the central boron atom. The donor−acceptor interaction energy is given by a second-order perturbation theory in NBO basis.[41] Using this treatment, the total donating energy of lone pairs on pyrrole N to central Mg in MgPc was calculated to be 129 kJ/mol, while no significant donation took place in the case of SubPc. The lack of electron donation in SubPc is attributable to the lack of electron-accepting orbitals in boron. Thus, at least some parts of the unstability of SubPc seems to be caused by a lack of donor−acceptor stabilization in the B−N (pyrrole N) bonds.

Is there any other reason for the reactivity of SubPc? To answer this question, the structure/energy changes accompanying elimination of the axial ligand (halogen, X) of SubPc (i.e., SubPc $\rightarrow$ $SubPc^+ + X^-$) were considered. Although this is not shown in a figure, the shape of the main skeleton of SubPc changes on elimination of the axial halogen atom, from a shuttlecock-shaped form to a more planar form, and the stabilization energy is about 100 kJ/mol. The NBO analysis has also indicated that cationic charge on the central boron atom is delocalized over the whole molecule, suggesting that the stability of a halogen-eliminated intermediate is high (the calculated cationic charge on B in $SubPc^+$ is only 0.277). From this, it is likely that the initial step of the ring expansion reaction consists of a dehalogenation process.

Finally, we attempted to obtain an approximate estimation of the reaction enthalpy. The ring expansion reaction of SubPc to form Pc can be written as SubPc + phthalonitrile $\rightarrow$ Pc. We make a rather bold estimation for this reaction by using MgPc, since boron-centered Pc does not exist. The DFT calculation gave formation energies of 1106.263, 366.483, and 1586.389 kJ/mol for SubPc, phthalonitrile, and MgPc, respectively, suggesting −113.642 kJ/mol for the enthalpy of the ring expansion reaction. Although this result is very approximate, the above value indicates that the reaction is exothermic and apt to proceed without supplying substantial heat.

VI. Band Deconvolution of the Spectral Envelopes of SubPc. It was suggested in the preceding section (V-i) that the Q-bands of SubPc are orbitally doubly degenerate. Accordingly, to verify this experimentally and to find the position (energy) and number of transitions to the degenerate excited states, the electronic absorption and MCD spectral envelopes of SubPc without peripheral substituent groups were deconvoluted simultaneously. The deconvolution results are shown in Figure 14 (the abscissa is expressed in wavenumber units), and the fitting parameters are summarized in Table 6. In the Q-band (16 500−22 000 cm^{-1}) and Soret band (22 000−40 000 cm^{-1}) regions, 13 and 9 bands are required in order to fill the absorption and MCD spectral envelopes. These numbers represent the minimum number required to obtain satisfactory fits and are slightly smaller than those required in the band

(39) Foster, J. P.; Weinhold, F. *J. Am. Chem. Soc.* **1980**, *102*, 7211. Reed, A. E.; Weinhold, F. *J. Chem. Phys.* **1985**, *83*, 1736. Reed, A. E.; Curtius, L. A.; Weinhold, F. *Chem. Rev.* **1988**, *88*, 899.

(40) Frisch, M. J.; Trucks, G. W.; Schlegel, H. B.; Gill, P. M. W.; Johnson, P. G.; Robb, M. A.; Cheeseman, J. R.; Keith, T.; Peterson, G. A.; Montgomery, J. A.; Raghavachari, K.; Al-Laham, M. A.; Zakrzewski, V. G.; Ortiz, J. V.; Foresman, J. B.; Cioslowski, J.; Stephanov, B. B.; Nanayakkara, A.; Challacombe, M.; Peng, C. Y.; Ayala, P. Y.; Chen, W.; Wong, M. W.; Andres, J. L.; Replogle, E. E.; Gomperts, R.; Martin, R. L.; Fox, D. J.; Binkley, J. S.; Defrees, D. J.; Baker, J.; Stewart, J. P.; Head-Gordon, M.; Gonzalez, C.; Pople, J. A. *Gaussian 94/DFT*; Gaussian Inc.: Pittsburgh, PA, 1995.

(41) Reed, C. A.; Weinhold, F.; Curtiss, L. A.; Pochatko, D. *J. Chem. Phys.* **1986**, *84*, 5687.

Table 6. Band-Fitting Parameters for SubPc in Chloroform

band no.	position, ν/cm^{-1} (λ/nm)	width,[a] $\Delta\nu$/cm^{-1}	band type	band no.	position, ν/cm^{-1} (λ/nm)	width,[a] $\Delta\nu$/cm^{-1}	band type
1	17 163 (583)	596	B	14	23 570 (424)	1755	B
2	17 581 (569)	448	B	15	25 475 (391)	1598	B
3	17 823 (561)	508	**A**	16	27 874 (359)	2203	**A**
	17 823 (561)	508	B		27 874 (359)	2203	B
4	18 210 (549)	591	B	17	30 036 (333)	2931	B
5	18 423 (543)	585	B	18	32 217 (310)	2250	B
6	18 808 (532)	584	B	19	33 193 (301)	3683	**A**
7	19 093 (524)	511	B		33 193 (301)	3683	B
8	19 410 (515)	560	B	20	36 164 (277)	3286	B
9	19 808 (505)	601	B	21	37 684 (265)	2150	**A**
10	20 314 (492)	617	B		37 684 (265)	2150	B
11	20 801 (481)	593	B	22	42 097 (238)	2659	B
12	21 305 (469)	544	B				
13	21 767 (459)	508	B				

[a] Width at half-height.

deconvolution of Pc's.[18,42] In the Q-band region, each MCD band was fitted with Faraday *B* terms, except for that corresponding to the Q_{0-0}-band. Attempts to replace this *A* term by two *B* terms of opposite sign significantly increased the residual noise, thus confirming that the Q_{0-0}-band corresponds to a transition to the orbitally degenerate state.

The Soret region is complicated by the presence of several overlapping bands of relatively equal intensity. Deconvolution identified three *A* terms at 359 (27 823 cm^{-1}), 301 (33 193 cm^{-1}), and 265 nm (37 684 cm^{-1}). Of these, the band at 359 nm corresponds to a weak shoulder on the long wavelength tail of what we call the Soret band. The presence of a similar small band has also been observed for Pc's around 370−430 nm.[42e] Since the intensity of this band is so weak, general MO calculations do not predict it. Judging from the intensity, position, and similarity to Pc systems, the *A* term located at 301 nm appears to be the B-band of this SubPc. The third *A* term at 265 nm may then be assigned to the N-band. As has been observed for Pc's, this *A* term is smaller than that at 301 nm.[18,42e]

VII. Time-Resolved EPR. To date, the time-resolved EPR (TREPR) technique has been used to investigate the extent of π-delocalization in the lowest excited triplet (T_1) state and the selectivity of the intersystem crossing (ISC) from the lowest excited singlet (S_1) state to the T_1 state.[43] Accordingly, the TREPR spectrum was recorded and discussed in comparison with that of a representative MtPc, i.e., ZnPc.

TREPR spectra of tBSubPc and tBZnPc are shown in Figure 15, together with their simulations, and the obtained EPR parameters are summarized in Table 7. The zero-field-splitting parameter, *D*, of tBSubPc is larger than that of tBZnPc. In general, *D* values originate from the magnetic dipolar−magnetic dipolar interaction and spin−orbit coupling (SOC). Since the deviations of the *g* values from the free-electron value (=2.0023) are so small (<0.002 and 0.005 for tBSubPc and tBZnPc, respectively), the contribution of the SOC can be neglected for both tBSubPc and tBZnPc.[44] Therefore, the *D* values must only be due to magnetic dipolar−magnetic dipolar interactions and denote the extent of π-delocalization in the T_1 state.[24a] From

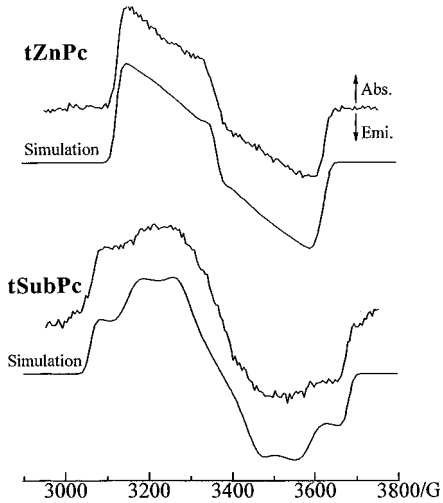

Figure 15. TREPR spectra of tBZnPc (top) and tBSubPc (bottom) with their simulations. These spectra were observed at 20 K and 0.5 μs after laser excitation.

Table 7. Zero-Field-Splitting Parameters and ISC Ratios Obtained from the Simulation

compd	*D*/GHz	*E*/GHz	Px:Py:Pz
tBSubPc	0.870	0.120	0:0.05:0.95
tBZnPc	0.705	0.215	0:0.10:0.90

the observed *D* values, the extent of π-delocalization in tBSubPc appears much smaller than that in tBZnPc in the T_1 state, and this result is consistent with the fact that the S_1 energy (~14 500 cm^{-1}) of tBZnPc is much lower than that (~17 500 cm^{-1}) of tBSubPc, due to the larger π-system in the former.

Our simulation reveals that the ISC from the S_1 to the T_{1z} sublevel is selective for tBSubPc. This selectivity in tBSubPc is similar to that in tBZnPc but is contrary to that in MgPc or H_2Pc.[45] The selective ISC in tBZnPc is reasonably interpreted by SOC due to the dπ atomic orbitals on the heavy zinc ion.[46] However, the contribution of the dπ atomic orbital on a central B atom of tBSubPc can be eliminated because of the energy difference. To clarify the origin of the selective ISC in tBSubPc, MO calculations were carried out using the AM1 Hamiltonian.[47] After geometrical optimization, configuration interactions (CIs)

(42) (a) Ough, E.; Gasyna, Z.; Stillman, M. J. *Inorg. Chem.* **1991**, *30*, 2301. (b) Mack, J.; Stillman, M. J. *J. Am. Chem. Soc.* **1994**, *116*, 1292; *J. Phys. Chem.* **1995**, *99*, 7935; *Inorg. Chem.* **1997**, *36*, 413. (d) Mack, J.; Kobayashi, N.; Leznoff, C. C.; Stillman, M. J. *Inorg. Chem.* **1997**, *36*, 5624. (e) Nyokong, T.; Gasyna, Z.; Stillman, M. J. *Inorg. Chem.* **1987**, *26*, 1087.

(43) Ishii, K.; Fujisawa, J.; Adachi, A.; Yamauchi, S. Kobayashi, N. *J. Am. Chem. Soc.* **1998**, *120*, 3152.

(44) (a) Kooter, J. A.; Canters, G. W.; van der Waals, J. H. *Mol. Phys.* **1977**, *33*, 1545. (b) Ishii, K.; Ohba, Y.; Iwaizumi, M.; Yamauchi, S. *J. Phys. Chem.* **1996**, *100*, 3839.

(45) Akiyama, K.; Tero-Kubota, S.; Ikegami, Y. *Chem. Phys. Lett.* **1991**, *185*, 65.

(46) van Dorp, W. G.; Schoemaker, W. H.; Soma, M.; van der Waals, J. H. *Mol. Phys.* **1975**, *30*, 1701.

(47) Dewar, M. J. S.; Zoebisch, E. G.; Healy, E. F.; Stewart, J. J. P. *J. Am. Chem. Soc.* **1985**, *107*, 3902.

were calculated to examine the electronic configurations in the S_1 and T_1 states. In the CI calculations, only electronic configurations whose eigenvalues were less than 8 eV were taken into account. The calculations have revealed that the contributions from the HOMO-to-LUMO transition are 97 and 85% for the T_1 and S_1 states, respectively, and that the E_x and E_y states are degenerate in both the S_1 and T_1 regions because of the degeneracy of the LUMOs (e_x and e_y). The SOC between the ^1E_y and ^3E_y states is negligibly small, so that coupling between the ^1E_x and ^3E_y states originating from that between the e_x and e_y MOs only is considered. From the values of coefficients of e_x and e_y MOs, it was found that the populations of the P_x and P_y orbitals are larger than that of the P_z orbital for both B and Br atoms. For example, the e_y MO coefficients of the B atom are −0.00003, −0.01903, 0.02853, and 0.00027 for 2S, $2P_x$, $2P_y$, and $2P_z$ orbitals, respectively. The e_y coefficients of the Br atom are, on the other hand, 0, −0.00587, 0.00882, and 0.00008 for the 4S, $4P_x$, $4P_y$, and $4P_z$ orbitals, respectively. Using the SOC constants of the B and Br atoms (11 and 2460 cm^{-1}, respectively[48]), the SOC on the B and Br atoms is estimated to be 0.013 and 0.28 cm^{-1}, respectively, indicating that the SOC on the Br atom is much larger than that of the B atom. Therefore, the selective ISC of tBSubPc can be reasonably interpreted by SOC on the axial Br atom.

Conclusions

A subazaporphyrin, subphthalocyanines, and a subnaphthalocyanine have been synthesized and characterized by various spectroscopic methods, including electronic absorption, MCD, fluorescence emission, and NMR. Both the Q-bands and Soret bands shift to longer wavelengths with concomitant increase in intensity, in the order of the above compounds, i.e., with increasing size of the π-conjugated system. Molecular orbital calculations have succeeded in reproducing the experimental data and have shown that the red-shift of the Q-band is due mostly to destabilization of the HOMO level. A 15-crown-5-ed subphthalocyanine does not dimerize following the addition of cations which induce dimerization of 15-crown-5-ed phthalocyanines. As an explanation of this, force field calculations have proposed a hemisphere structure with three crown ether voids standing like fences. Hitherto accumulated data on induced circular dichroism of cyclodextrin−chromophore complexes has suggested complexation of an axial ligand of crowned subphthalocyanine and 2,6-dimethyl-β-cyclodextrin. In the presence of isoindolediimine, subphthalocyanines experience ring expansion reactions to monosubstituted type phthalocyanines. To attain good yields, mixed solvent systems of DMSO and chloronaphthalene (or aromatic solvents such as toluene and *o*-dichlorobenzene) (3:1−1:2 v/v) are recommended at a reaction temperature of ca. 80−90 °C and a reaction time of almost 1 day. The Q-bands of the resultant monosubstituted type phthalocyanines split into two and shift to longer wavelength with increasing size of the fused aromatics. In these low-symmetrical phthalocyanines, both the quantum yields and lifetimes of fluorescence emission become smaller with the departure of symmetry from D_{4h}. Comparison of experimental spectra and the results of molecular orbital calculations has suggested that two pyrrole protons are linked at pyrrole nitrogens along the short axis. Band deconvolution analysis of the electronic absorption and magnetic circular dichroism spectra of unsubstituted subphthalocyanine locates four transitions to degenerate excited states at 561, 359, 301, and 265 nm. The values of the zero-field-splitting parameter in the time-resolved EPR spectra indicate that the π-system of the subphthalocyanines is, indeed, smaller than that of the phthalocyanines.

Experimental Section

(i) Measurements. Solvents for spectroscopic measurements, *o*-dichlorobenzene (Aldrich, Gold label), acetonitrile, and chloroform (Wako, Spectrograde) were used as supplied.

The 400-MHz ^1H NMR and IR spectral measurements were made with JEOL GSX-400 and Shimadzu FTIR-8100M spectrometers, respectively. To eliminate the effect of aggregation, the concentration of the samples for NMR was ca. 0.1 mM, unless otherwise noted. Electronic spectra were recorded with a Shimadzu UV-250 spectrometer. MCD spectra were run on a Jasco J-500 spectrodichrometer equipped with a data processor and with an electromagnet which produced magnetic fields up to 1.17 T, with parallel and then antiparallel fields. Its magnitude was expressed in terms of molar ellipticity per tesla, $[\theta]_M/10^4$ deg mol^{-1} cm^{-3} cm^{-1} T^{-1}. CD spectra were recorded on a Jasco J-720 spectrodichrometer in acetonitrile and acetonitrile−water (3:2 v/v) in the presence of DMβCDx (Nacalai) at 20 °C. Fluorescence spectra were obtained with appropriate filters to eliminate scattered light. Fluorescence quantum yields (ϕ_F) were determined by the use of quinine sulfate in 1 N H_2SO_4 ($\phi_F = 0.55$ at 296 K), free base tetraphenylporphyrin in benzene ($\phi_F = 0.11$), Rhodamine B in ethanol ($\phi_F = 0.97$), ZnPc ($\phi_F = 0.30$), and H_2Pc ($\phi_F = 0.60$) in CNP as standards.[26] The ϕ_F value of SubNc alone was obtained using the ϕ_F value of compound PyPc ($\phi_F = 0.54$ in *o*-dichlorobenzene) as a new standard. Data were obtained by a comparative calibration method, using the same excitation wavelength and absorbance for the azamacrocycles, unsymmetrical Pc analogues, and calibrants, and the same emission energies. Fluorescence decay curves were obtained at 20 °C by a Horiba NAES-550 series, using combinations of glass filters and a monochromator for monitoring the emission. The lifetimes were determined from the decay curves by the use of the least-squares method. All solutions for fluorescence measurements were purged with argon before measurements.

TREPR measurements were carried out at 20 K on a Bruker ESP 300E spectrometer using an Oxford ESR 900 cold gas flow system.[24a] Samples were excited at 585 nm by a Lumonics HD-500 dye laser pumped with a Lumonics EX500 excimer laser. The TREPR signals from the EPR unit were integrated by a LeCroy 9450A oscilloscope. For TREPR measurements, toluene was used as solvent, and samples were deaerated by the freeze−pump−thaw method.

(ii) Synthesis. **(a) tBSubPc.** We reported this compound in our previous communication.[1]

(b) SubAP. A 0.81-mL portion of a 1,2-dichloroethane solution of 1 M tribromoboron (0.81 mmol) and 1-(1,2,2-tricyanoethenyl)-2-trifluoromethylbenzene (600 mg, 2.43 mmol) were heated in chlorobenzene (1.5 mL) at 80 °C under nitrogen for 1 h. After cooling, the crude product was imposed on a preparative TLC column of alumina using chloroform as eluent, and the yellow fraction with $R_f = 0.27$ was collected and extracted using the same solvent. Evaporation of the solvent, followed by recrystallization from chloroform−hexane, afforded 4.2 mg (1.9%) of the desired triazasubporphyrin. FAB mass (*m*/*z*): 752 (M − Br). Anal. Calcd for $C_{36}H_{12}N_9BF_9$: C, 51.96; H, 1.45; N, 15.15. Found: C, 51.13; H, 1.82: N, 14.03. ^1H NMR ($CDCl_3$, 500 MHz): δ 7.49 (m, 3H, arom), 7.63−7.77 (m, 6H, arom), 7.87 (m, 3H, arom). UV−vis ($CHCl_3$; λ_{max} (10^{-4} ϵ)): 411 (1.22), 255 (2.70).

(c) SubNc. 2,3-Dicyanonaphthalonitrile (1.87 g, 10.5 mmol) was dissolved in 12 g of 2,3-dimethyl-6-*tert*-butylnaphthalene at 80 °C under nitrogen. Tribromoboron (1.33 g, 5.3 mmol, 0.5 mL) was added slowly, and the temperature was maintained at ca. 180 °C for ca. 15 min. As the reaction proceeded, the color of the solution changed from green to dark blue. After the solution was cooled to room temperature, 120 mL of carbon tetrachloride and 40 mL of hexane were added, and the resultant precipitate was collected by filtration and washed with 20 mL of carbon tetrachloride twice. A portion of the residue was taken and applied to alumina column chromatography (Act. VI) using

(48) Goodman, B. A.; Raynor, J. B. Electron Spin Resonance of Transition Metal Complexes. In *Advances in Inorganic Chemistry and Radiochemistry*; Emeleus, H. J., Sharpe, A. G., Eds.; Academic Press: New York, 1970; Vol. 13.

methylene chloride−pyridine (1:1 v/v) as eluent. The first-eluted blue band was collected, recrystallized from toluene, and used for elemental analysis. Most of the residue was transferred to a Soxhlet apparatus and extracted by toluene under a nitrogen atmosphere. Toluene was evaporated from the extract to some extent to induce crystallization, to afford, after cooling, 2.28 g (34.6%) of dark blue crystals. Anal. Calcd for $C_{36}H_{18}N_6BBr$: C, 69.15; H, 2.90; N, 13.44. Found: C, 68.42; H, 3.50: N, 12.17. This compound may be unstable in alcohol and DMSO, since the color of the solution changed following the addition of these solvents. UV−vis (DCB; λ_{max} (10^{-4} ϵ)): 667 (6.26), 608 (2.06), 328 (3.09), 302 (4.62).

(d) SubCRPc. 2,3-(3′,4′-Dicyanobenzo)-1,4,7,10,13-pentaoxacyclopentadeca-2-ene, the so-called 15-crown-5-ed phthalonitrile (1.59 g, 5 mmol),[16] triphenylboron (0.412 g, 1.7 mmol), and 1,8-diazabicyclo-[5,4,0]-7-undecene (DBU) (0.25 g, 1.7 mmol) in naphthalene (5 g) were heated at 218 °C for 15 min. After the solution was cooled to room temperature, the residue was imposed on a silica gel column using chloroform−methanol (20:1 v/v) as eluent. The reddish-purple fraction was collected, and the solvent was removed using an evaporator. The residue was redissolved in a small amount of chloroform and chromatographed on an alumina column (Act. I), followed by a gel permeation column (Bio-beads SX-2, Bio-Rad) using chloroform as eluent. Evaporation of the solvent, followed by recrystallization from ethyl acetate−methanol, gave ca. 7 mg (0.4%) of reddish-purple solid of the desired compound. FAB mass (*m*/*z*): 1042 (M^+, 100), 965 ($M^+ - C_6H_5$, 18). Anal. Calcd for $C_{54}H_{59}N_6O_{15}B$: C, 62.19; H, 5.70; N, 8.06. Found: C, 61.30; H, 6.25: N, 7.52. ^{1}H NMR ($CDCl_3$, 500 MHz): δ 8.19 (s, 6H, arom), 6.70 (t, J = 7.6 Hz, 1H, arom), 6.58 (t, J = 7.6 Hz, 2H, arom), 5.40 (d, J = 7.6 Hz, 2H, arom), 4.45−4.53 (m, 6H, aliph), 3.73−3.86 (m, 24H, aliph). UV−vis ($CHCl_3$; λ_{max} (10^{-4} ϵ)): 569 (5.32), 326 (3.56), 275 (4.72).

(e) (tBSubPc)$_2$O. The axial ligand (Br) of tBSubPc (210 mg, ca. 0.33 mmol) was changed to an OH group according to the literature,[7] by using an ion-exchange resin (the IR absorption band seen at 890 cm^{-1} (assignable to a B−Br bond) of tBSubPc disappeared in this process). The resulting tBSubPc having an OH group was dissolved in 2−3 mL of nitrobenzene containing a small amount of molecular sieves (4 Å) and heated under reflux for 6 h under nitrogen. The solvent was removed under reduced pressure, and the residue was imposed onto a basic alumina column (Act. III, $3^{\phi} \times 10$ cm^{-1}) using methylene chloride as eluent. A front-running reddish-purple portion with R_f = 0.97 was collected and further purified using gel permeation columns (Bio-beads SX-2, Bio-Rad) to give 8.8 mg (4.7%) of the desired (tBSubPc)$_2$O. FAB mass (*m*/*z*): 1143 (M + 1). Anal. Calcd for $C_{72}H_{72}N_{12}OB_2$: C, 75.66; H, 6.35; N, 14.70. Found: C, 75.30; H, 6.56: N, 14.25. ^{1}H NMR($CDCl_3$, 500 MHz): δ 8.64 (m, 6H, arom), 8.48 (m, 6H, arom), 7.78 (br, 6H, arom), 1.25 (br, 54H, aliph). UV−vis ($CHCl_3$; λ_{max} (10^{-4} ϵ)): 538 (3.06), 307 (2.63), 264 (3.25). This compound is unstable on silica gel or alumina and decomposes after 3−4 h.

(f) Monosubstituted Type Pc Compounds NilPc−PyPc. Synthesis of NilPc−AnPc was reported previously.[1] PyPc was prepared similarly as a dark blue solid from 257 mg (0.4 mmol) of tSubPc and crude Py obtained from 360 mg (2.8 mmol) of 2,3-dicyanopyridine and ammonia gas.[49] Yield: 71 mg (26%). Mass (*m*/*z*): 683 (M^+). Anal. Calcd for $C_{43}H_{41}N_9$: C, 75.52; H, 6.04; N, 18.43. Found: C, 75.28; H, 6.30; N, 18.17. ^{1}H NMR ($CDCl_3$, 500 MHz): δ 7.7−8.5 (m, 6H, arom), 8.6−9.6 (m, 6H, arom), 1.78−1.90 (m, 27H, aliph), −2.3 to −2.8 (2 br s at −2.43 and −2.64, 2H, pyrrole H). UV−vis−near-IR (DCB; λ_{max} (10^{-4} ϵ)): 688 (11.70), 659 (8.28), 635 (3.10), 605 (2.15), 343 (5.24).

(ii) Computational Method. The structures of phthalocyanine analogues were constructed by using X-ray structural data[50] of standard phthalocyanine, naphthalene, and anthracene and by making the rings perfectly planar and adopting the C_{2v} symmetry. Molecular orbital (MO) calculations were performed for dianions of subazamacrocycles and neutral protonated species of low-symmetrical Pc analogues within the framework of the PPP approximation,[36] where the semiempirical parameters which were recommended in a literature[51a] were modified.[38] The use of the latter parameters gave slightly better results. For the calculation of (pyrrole proton) deprotonated dianions, these are atomic valence state ionization potentials of 11.16 (carbon), 20.21 (central nitrogen), and 14.12 eV (imino nitrogen), together with atomic valence state electron affinities of 0.03 (carbon), 5.32 (central nitrogen), and 1.78 eV (imino nitrogen). In the case of protonated neutral species, the values of atomic valence state ionization potentials and electron affinities of the central nitrogens are either 27.3 and 16.44 (protonated nitrogen) or 17.0 and 13.84 eV (nonprotonated nitrogen). For (pyrrole proton) deprotonated species, the central nitrogen atoms were assumed to be equivalent, supplying 1.5 electrons each to the π-system, while the electron density at the central nitrogens of neutral protonated species were fixed at 1.15 (nitrogens not bonding proton) and 1.85 (nitrogens bonding proton). In addition, σ polarizability was taken into account according to Hammond.[51b] Resonance integrals were taken to be −2.48 (β_{CN}) and −2.42 eV (β_{CC}).[51a] Two-center electron repulsion integrals were computed by the method of Mataga and Nishimoto.[51b] The choice of configurations was based on energetic considerations, and all singly excited configurations up to 48 393 cm^{-1} (6 eV) were included. In the calculation of formation, bonding, and donation energies, the *ab initio* MO program package Gaussian94/DFT[40] was employed with NBO analysis.[39] In the section entitled Origin of the Reactivity of SubPc for the Ring Expansion, optimized structures were used throughout with the B3LYP DFT method and the 6-31G basis set.[40] Geometry optimization on SubCRPc with three sodium cations was performed using the UNIVERSAL 1.02 force field[52] on a Program Package Cerius2, to minimize the total energy of the cation-bound SubCRPc molecule.

Acknowledgment. We thank Ms. R. Kondo and Dr. S. Nakajima for carrying out preliminary studies, and we gratefully acknowledge financial support from the Asahi Glass and Mitsubishi Foundations. We also thank Prof. M. J. Stillman for donation of his band deconvolution program.

JA983325C

(49) Cook, A. H.; Linstead, R. P. *J. Chem. Soc*. **1937**, 929.

(50) Robertoson, J. M.; Woodward, I. *J. Chem. Soc.* **1937**, 219. Barrett, P. A.; Dent, C. E.; Linstead, R. P. *J. Chem. Soc.* **1936**, 1719. Brown, C. J. *J. Chem. Soc. A* **1968**, 2488, 2494. Kirner, J. F.; Dow, W.; Scheidt, D. R. *Inorg. Chem.* **1976**, *15*, 1685.

(51) (a) Tokita, S.; Matsuoka, K.; Kogo, Y.; Kihara, K. *Molecular Design of Functional Dyes—PPP MO Method and Its Application*; Maruzene: Tokyo, 1990. (b) Hammond, H. *Theor. Chim. Acta* **1970**, *18*, 239. (c) Mataga, N.; Nishimoto, K. *Z. Phys. Chem. (Frankfurt am Main)* **1957**, *13*, 140.

(52) Rappe, A. K.; Casewit, C. J.; Colwell, K. S.; Goddard, W. A., III; Skiff, W. M. *J. Am. Chem. Soc.* **1992**, *114*, 10024.